Spontaneous and induced emission of a Rydberg atom in a cavity

I. M. Beterov and P. B. Lerner

Institute of Thermal Physics, Siberian Branch of the Academy of Sciences of the USSR, Novosibirsk and P. N. Lebedev Physics Institute of the Academy of Sciences of the USSR

Usp. Fiz. Nauk **159**, 665–712 (December 1989)

Experimental and theoretical studies of Rydberg masers–quantum-electronic devices which produce and employ microwave radiation from highly excited atoms in a cavity–are reviewed. The experimental results are based mainly on studies performed by S. Haroche's group in Paris and H. Walther's group in Munich. In contradistinction to the usual quantum generators the quantum properties of the electromagnetic field itself play an important role in the analysis of the behavioral dynamics of Rydberg masers. The most striking results obtained in this field are the discovery of "quantum revival" and the achievement of maser generation on two-photon transitions and Fok states of the electromagnetic field.

I. INTRODUCTION

The real revolution brought about in macroscopic quantum physics in the last few years by experiments with Rydberg atoms[1-9] is explained by the fact that the extremely high polarizability ($\sim n^2$), long lifetimes ($\tau \sim n^3$ for $l \sim 1$ and $\tau \sim n^5$ for $l \leqslant n$), the strong field effects (the dynamic Stark shift $\sim n^7 l^5$ and the Zeemann effect $\sim n^4$) in contradistinction to nonlinear optics make it possible to realize exotic regimes of interaction with the electromagnetic field under conditions when the number of photons is small, the number of atoms is small, and correspondingly the intensities of the external fields are negligible. In addition, on an atomic scale, because nonlinear effects depend strongly on the principal quantum number not only can the field itself be strong but its quantum or thermal fluctuations may be large. This makes it possible to observe a number of new phenomena, associated with the stochastic characteristics of the field as such and not with the chaos introduced by the mode structure of the field, etc., as happens in nonlinear optics. The interaction of Rydberg atoms with the quantum field of a cavity can serve as a basis for the development of a new class of quantum-electronic devices. The working medium in such devices is a small number of highly excited atoms. An important aspect of this rapidly progressing area of experimental methods is the possibility of detecting microwave radiation at the quantum level of sensitivity.

The objective capability of working with Rydberg states (RSs) has been made possible by the following achievements in experimental technique: 1) the development of tunable dye lasers and semiconductor lasers with adequate power and a narrow spectral line, which have made it possible to obtain atoms excited in a cascade fashion into a Rydberg state with a given value of n; 2) the development of experimental techniques for working with very rarefied atomic and molecular beams; and 3) the development of superconducting cavities with extremely high quality factors of up to $Q = 19^9$ in the range of transitions characteristic for RSs (tens and hundreds of GHz).

It is very important to note that many effects of "low-energy quantum electrodynamics," such as, the appearance of spontaneous emission,[1,10] nondissipative decay of Rabi oscillations in the quantum field of a resonator ("Cummings collapse"[4,11] and "Dicke subemission"[7,12]) were predicted long before experiments were performed and, moreover, when concrete physical systems and the region of parameters in which the theory can be checked were not yet known clearly. The properties of a "one-atom"[1] or two-photon maser[9] which permit observing subtle effects associated with the quantum properties of the photon field in the microwave range, are undoubtedly interesting.

Rydberg amplifiers (masers) also function in space.[13,14] A number of astrophysical processes occurring in interstellar gas, which interacts with the remnants of supernova explosions, collisions between interstellar clouds, and supersonic gas flows accompanying the formation of stars result in the formation of RSs with very large values of n, as high as $n = 1000$[15]. The functioning of Rydberg masers in space results in the amplification of the spectral lines of stars and quasars in the radio range.

The rapid development of the aspect of the subject pertaining to the spontaneous and induced emission of a Rydberg atom in a cavity which is of interest from the applied and fundamental viewpoints, makes it impossible to give a complete picture of the progress achieved, but the discovery of the effects presented is a triumph of modern experimental techniques and the methods of macroscopic quantum electrodynamics.

The main properties of highly excited states and a number of specific problems associated with them have been discussed in a special monograph[16] and reviews[17,18], and we shall not discuss them in detail. Only the dependences of the natural lifetimes of the RSs are not clear. For the case $l \sim 1$, $n' \ll n$, $\langle r_{nn'} \rangle^2 \sim n^{-3}$, $A_{nn'} \sim n^{-3}$ [16], and $\nu_{nn'}$ is of the order of unity in atomic units. For $n' \sim n$, $\langle r_{nn'} \rangle^2 \sim n^4$, $\nu_{nn'} \sim n^{-3}$ and $A_{nn'} \sim n^{-5}$.

For the low-lying states their overlap integral with RSs with high values of the angular momentum decreases much more rapidly. This is easy to understand[19], based on the fact that for highly excited states the region of motion of the Rydberg electron at the perihelion makes the main contribution to the transition matrix element. Unlike strongly elongated electron orbits with $l \sim 1$ and $n \gg 1$ the wave function of states with $l \lesssim n$ looks like a narrow ($\Delta r/r \sim n^{-1}$) toroid and the overlap integral decreases more rapidly than for states with small values of l. For states with $l \lesssim n$ transitions into states with $l' \lesssim n'$ and $n' < n$ are characteristic. The long

 0038-5670/89/121084-27$01.80

TABLE I. The characteristic lifetimes of Rydberg states of the sodium atom (in ns) taking into account thermal radiation[23]

Level	0 K	410 K	600 K	Calculation of Ref. 22	Experiment of Ref. 144
$11P_{1/2}$	10 025	3 799	2 124	11 232	
$11P_{3/2}$	11 388	4 876	3 563	»	
$12P_{1/2}$	13 407	4 417	3 149	15 048	3.5±1 мс
$12P_{3/2}$	15 639	5 895	4 292	»	
$13P_{1/2}$	17 472	5 046	3 583	19 664	4.7±1.2 мс
$13P_{3/2}$	20 791	7 020	5 091	»	
$14P_{1/2}$	22 286	7 598	5 534	25 148	5.5±1.5 мс
$14P_{3/2}$	26 918	8 242	5 960	»	
$20P_{1/2}$	73 653	21 033	15 538	81 007	
$20P_{3/2}$	89 736	22 263	16 261	»	
$30P_{1/2}$	—	—	—	299 398	
$36P_{1/2}$	—	—	—	535 956	

lifetimes and the strongly anisotropic polarizability of such states make them very important for experiments.[9]

The radiation width in a blackbody radiation field is also important for preserving atoms in highly excited states.[16] Namely, $B_{nn'} = \bar{n}_T A_{nn'}$, where $\bar{n}_T$ is the average number of blackbody photons per mode. For $\hbar\omega \ll kT$ the Rayleigh–Jeans law specifies that $\bar{n}_T \sim n^2 \sim \nu^6$, which gives $\tau \sim n^{-2}$.

Transitions induced by blackbody radiation thus seriously restrict the lifetime of states with large values of n. The way out of this situation is to use in high-precision experiments with RSs a helium cryostat, which, for example, is an intrinsic part of the setup employed in Ref. 8. The sensitivity of RSs to external fields (Table 1) makes it necessary to screen Rydberg masers very carefully from external fields.

We shall summarize, following Ref. 19, the basic spectroscopic considerations which much be kept in mind when working with highly excited states:

1) the Rydberg electron is a good tool for studying the intra-atomic potential by measuring the quantum defect as well as the fine and hyperfine splitting;

2) the effect of radiation on highly excited atoms differs substantially from the effect of radiation on states of low excitation; maser generation can occur on a small number of atoms;

3) the binding energy of the electron with the atomic core is very small; and,

4) because of their large sizes and low binding energies Rydberg atoms exhibit peculiar characteristics in collisions: a large and loose atom is almost transparent to a compact particle (neutral atom or ion) interacting with it via induced polarization.

Collisions with electrons are also modified. For highly excited states the interaction cross section is close to that for free-face electron scattering; the low value of this cross section ensures that the RS will be quite stable up to $n \approx 1000$ in an interstellar gas.[20] A Rydberg maser consists of the system "Rydberg atoms + cavity." The use of a high-Q microwave cavity creates feedback between the radiation and the external field acting on the atoms. The existence of feedback radically changes the characteristics of the radiation associated with RSs.

This review is devoted precisely to those aspects of the radiation from a system of RSs that depend strongly on the interaction of the atoms with the microwave fields which arise in the course of generation, detection, and other electrodynamic processes which are typical for quantum-electronic devices.

II. THE SPECTROSCOPY OF RYDBERG STATES

To study the interaction of highly excited states with an electromagnetic field it is first necessary to know how to prepare these states with given quantum numbers, in particular, with very high values of n. Stepped laser excitation is the most precise method for obtaining Rydberg atoms; this method makes it possible to prepare such atoms in states with low values of the angular momentum (owing to the selection rules for dipole transitions). Combining laser excitation with quasistatic electric fields makes it possible to obtain circular atomic states which are important for metrological applications owing to their long lifetimes and insensitivity to external fields. Analogous methods are employed to prepare electropolarized (elongated) states one of whose parabolic quantum numbers is equal to zero. Such states provide a model of a one-dimensional hydrogen atom, and their wave function is concentrated in a narrow cone on one side of the ionic core. Second, one must know how to analyze such states: the population and in some cases the phase of the dipole moment (Ramsey's spectroscopic scheme). Stark spectroscopy of highly excited states is a powerful spectroscopic tool.

Third, the study of the spectroscopy of highly excited states is of interest in its own right, in particular, the theory of quantum defects and comparing this theory with experiment and the study of the mechanisms of broadening in a rapidly varying electromagnetic field. However these problems are only peripherally related with the subject of this review and they will be discussed in Secs. 7 and 8 in connection with the problems involved in building a radiometer in the "Rydberg atoms + cavity" system. The problem of the nonlinear polarization of Rydberg atoms is of fundamental importance. This rapidly developing field of the spectroscopy of highly excited states also falls outside the scope of this review, but we feel that it is necessary to present an annotated list of the latest investigations.

The use of Rydberg atoms for metrology and detection of microwave radiation is a very important practical problem. In spite of the quite good progress that has been made in

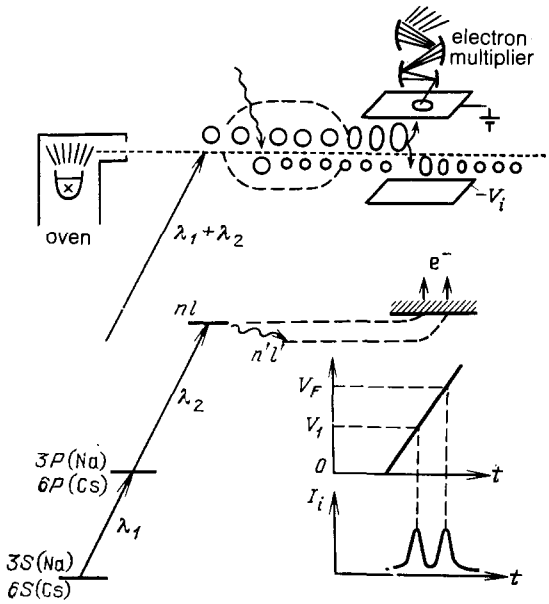

FIG. 1. Diagram illustrating the excitation and detection of Rydberg atoms.[58]

experimental techniques the problem of building real standards and the highly precise measurement of physical constants based on the shifts and broadening of Rydberg states are problems for future work.

1. The excitation and detection of Rydberg atoms. The following groups currently have the experimental setups required for studying the interaction of a beam of thermal Rydberg atoms with a microwave field: S. Haroche (France, Center for Microwave Spectroscopy, École Normal, Paris),[5] H. Walther (West Germany, Munich University),[1] T. F. Gallagher (Physics Laboratory of the University of Virginia[8]), and D. Kleppner (Massachusetts Institute of Technology, USA).[6] In the last few years research on the detection of a superradiant cascade in a medium with RSs has also been performed by Leonard's group at Hannover Technical University (West Germany). In the Soviet Union such a setup has been built at the Institute of Thermal Physics of the Siberian Branch of the Academy of Sciences of the USSR. Since most experiments have been performed using alkali metal atoms the general features of the experimental setups employed for obtaining highly excited states of atoms, including also for Rydberg masers, are virtually identical and differ by the types of lasers employed, the specific operating regimes, the characteristics of the recording apparatus, and the signal processing techniques. The setups employed by P. Koch's group (New York University, USA[29]), in which fast Rydberg atoms were obtained by means of charge-exchange collisions between protons and target molecules, are somewhat of an exception. Figure 1 shows a characteristic arrangement for preparing and detecting alkali-metal Rydberg atoms. The atomic beam is obtained by effusion from a heated oven (the oven temperature is typically 300–600 K depending on the element employed (Na, K, Pb, or Cs)) and propagates into a vacuum chamber with a residual gas pressure $< 10^{-6}$ torr. The density of atoms in the ground state in the interaction zone reaches values of $\sim 10^7$–10^9 cm^{-3}, though a number of experiments have also been performed with significantly lower densities (10^5 cm^{-3} and lower). Since the cross sections of collisional processes involving Rydberg atoms are large the choice of atomic density in the beam is important, since it determines the conditions of interaction of the Rydberg atoms with the radiation and the lifetimes of the atoms. The divergence of the atomic beams is not important and is usually equal to 10^{-2}–10^{-3} rad.

The region of interaction and detection is chosen depending on the operating regime of the lasers which selectively excite the atoms into the Rydberg states. Under conditions of continuous (steady-state) excitation the zone of interaction with the pump radiation is, as a rule, separated by quite a large distance from the zone of detection of the Rydberg atoms. The upper limit of this distance is determined by the lifetime of the prepared Rydberg atoms. As is well known, this lifetime is directly related with the value of the effective principal quantum number and it depends on the type of element, the presence of thermal radiation and its temperature, and the contribution of collisional quenching to the lifetime of the excited states which limits the mean free path (range) of the Rydberg atom in the evacuated volume. The effective lifetime τ_{eff} is determined by the relation

$$\tau_{\text{eff}}^{-1} = \tau_{\text{R}}^{-1} + \tau_{\text{c}}^{-1}, \tag{1.1}$$

where τ_{R} is the radiative lifetime and τ_{c} is the collisional lifetime. The spontaneous lifetime can be estimated by the approximate formula[22]

$$\tau_{\text{R}} \approx \tau_0 n^{\alpha}. \tag{1.2}$$

For example, for Na $\tau_0 = 8.35$ nsec and $\alpha = 3.11$. Table I gives the computational results obtained for the radiative lifetimes of the Rydberg states of Na with the formula (1.2). It is obvious that starting with $n > 20$ the radiative lifetime exceeds ~ 10 μsec. Since the mean-free path is $l \sim v_{\text{at}} \tau_{\text{eff}}$, in the absence of collisional quenching for $v_{\text{at}} \sim 10^5$ cm/s and $\tau_{\text{eff}} \sim 10$ μs $l \gtrsim 1$ cm and increases as τ_{eff} increases. On the other hand calculations performed in different studies, for example, in Ref. 23, show that the presence of thermal radiation owing to, for example, the walls of the chamber or the oven, appreciably shortens the lifetime of Rydberg atoms as a result of induced radiative transitions and photoionization. The lifetime now depends on the temperature of the walls, the nature of its dependence on the principal quantum number of the excited state changes, etc. The computational results for the radiative lifetimes for Na taking thermal radiation into account are given in column 2 of Table I. One can see that at room temperature T $\sim$ 300 K the lifetimes are on the average three to four times shorter. An analogous picture is observed for atoms of other alkali metals.

Thus in order to separate the regions of excitation and detection the walls of the working chamber must in most cases be cooled to a quite low temperature, the temperature of liquid nitrogen ($T = 77$ K) or liquid helium (4 K). Cooling usually also improves the vacuum in the experimental chamber, thereby reducing the importance of collisional quenching of Rydberg atoms by the residual molecular gases. The rate of collisional quenching by impurities is largest in the case of electronegative molecules [$K_c \sim 10^{-7}$ -10^{-6} cm^{-3} s^{-1} (Refs. 24 and 25)], when quenching is accompanied by ionization of the Rydberg atom by the electron-transfer mechanism $A^* + M = A^+ + M^-$. Since

$$\tau_{\text{c}} = (k_{\text{c}} N_M)^{-1}, \tag{1.3}$$

where N_M is the density of quenching molecules, this mechanism of quenching becomes significant already for $N_M \approx 10^{11}$–10^{12} cm^{-3}, i.e., the residual-gas pressure should not exceed 10^{-6}–10^{-7} torr.

The situation becomes somewhat simpler when the Rydberg states are excited by short laser pulses ($\tau \approx 10^{-9}$–10^{-7} s). In this case at the end of the excitation pulse we have a bunch of diverging Rydberg atoms. They can be detected with the help of field ionization in a pulsed electric field.[26,27] If the highly excited atoms are in a microwave cavity, then pulsed generation can be achieved. In this case the lifetime must meet stricter requirements. However the duration of the pulse of microwave generation itself is determined in this case by the emergence time of the atoms from the cavity.

Experimental setups in which atoms in states with large values of the principal quantum number are prepared efficiently with the help of existing lasers are usually of greatest interest. In the case of alkali-metal atoms two- or three-step excitation is most often employed, though direct excitation with ultraviolet radiation is undoubtedly simplest. For example, in Ref. 28 the wavelength of the tunable dye laser radiation employed for excited Na or Cs at the first step [from the 3S or 6S ground state into the first excited state $3P_{3/2}$ (Na) and $6P_{3/2}$ (Cs)] was equal to 5896 Å for Na and 8521 Å for Cs. The excitation of nS and nD states from $P_{3/2}$ states was performed at wavelengths of 4110 Å (Na) and 5100 Å (Cs), respectively. The durations of the excitation pulses (5–10 ns) and the pulse repetition frequencies (5–10 Hz) were determined by the parameters of the pump-laser radiation. The tunable dye lasers were pumped either with a nitrogen (N_2) ultraviolet laser ($\lambda = 3377$ Å) or the second ($\lambda = 5320$ Å) and third ($\lambda = 3365$ Å) harmonics of the Nd:YAG lasers. The first step was saturated with power densities of the order of 1 kW/cm^2. At the second step the lasers permitted the excitation of approximately 10^6 atoms per pulse. Figure 2 shows a diagram of the three-step excitation of Rydberg states of the Na atom using an LiF:F_2^- color center laser; this scheme was implemented by Beterov *et al.*[24,25]

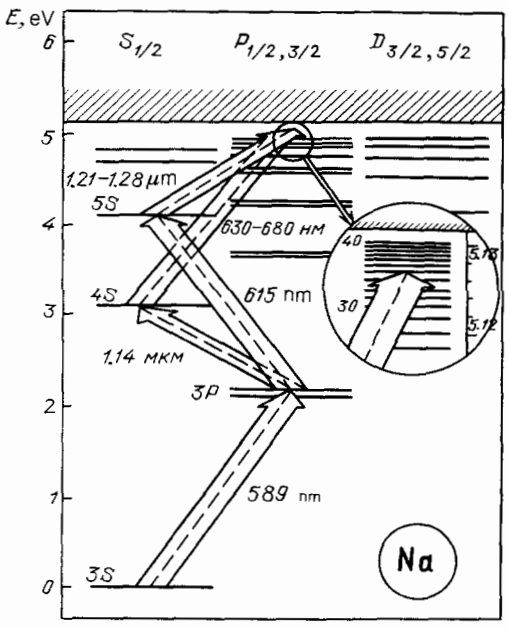

FIG. 2. Diagram of the energy levels of Na and transitions for three-step excitation of the Rydberg nP series.[24]

Since the radiative lifetime of the intermediate resonance level is short (for example, for Na $\tau \approx 1.6 \times 10^{-8}$ s) the short excitation pulses must be precisely synchronized in time. This is usually achieved by using the same laser to pump the dye lasers as well as by adjusting the optical propagation paths of the laser radiation. In the case of excitation with cw lasers such problems, naturally, do not arise.

The selectivity of the excitation of a Rydberg atom with a definite value of n is determined primarily by the ratio of the linewidth of the laser radiation at the last (second or third) step and the width of the absorption line. Since the excitation wavelength lies, as a rule, in the visible or near-IR regions of the spectrum the ratio of the Doppler and natural widths of the transition is important. The natural linewidth is determined by the relation

$$\Delta\nu_N \approx \frac{1}{2\pi}(\gamma_0 + \gamma_R), \tag{1.4}$$

where γ_0 and γ_R are the rates of decay of the lower working and Rydberg levels, respectively. As a rule, the lower working level is short-lived and it decays at a rate $\gamma_0 \approx 10^7$–10^8 s^{-1}, while at the low pressures characteristic for experiments with Rydberg masers the Rydberg states have rates of decay $\gamma_R < 10^6$ s^{-1}. As the vapor pressure is increased highly excited atoms relax primarily by the mechanism of collisional quenching by the intrinsic or buffer gas, so that the situation can change. Thus it can be assumed that $\Delta\nu_N \approx 10^7$–10^8 Hz.

In the case when the atomic beam propagates in a direction perpendicular to the exciting light field the Doppler linewidth is determined by the simple relation

$$\Delta\nu_D^n \approx \Delta\nu_D\theta = \frac{2\pi}{\lambda}\left(\frac{2kT}{M}\right)^{1/2}\theta, \tag{1.5}$$

where $\Delta\nu_D$ is the Doppler width of the absorption line on the exciting transition in the beam source and θ is the divergence of the atomic beam. For example, for sodium with $\lambda \sim 420$ nm and $T \approx 500$ K $\Delta\nu_D \approx 2$ GHz. For beam divergence $\theta \approx 10^{-2}$–10^{-3} the transverse Doppler width is $\Delta\nu_D'' \approx 20$–2 MHz, which is comparable to the natural linewidth. Thus it may be assumed that the width of the absorption line at the last step of excitation is < 10–100 MHz. When pulsed lasers with a pulse duration of 10^{-8}–10^{-9} s are employed for excitation of Rydberg atoms the radiation spectrum, in the best case, is determined by the Fourier transform of a single pulse, and the width is inversely proportional to the duration of the pulse and is much greater than the width of the absorption line in the beam. This is what limits the selectivity of excitation of Rydberg states with an increase in the principal quantum number n. For cw lasers it is now difficult to obtain a lasing line-width < 1–10 MHz. In this case the width of the absorption line fundamentally limits the quantum number n of the selectively excited state. The solution is preexcitation of Rydberg atoms into a state with an average principal quantum number $n \approx 10$–11, followed by irradiation with a narrow-band CO_2 laser with Stark tuning into resonance, as done in experiments performed by Koch[29] with beams of

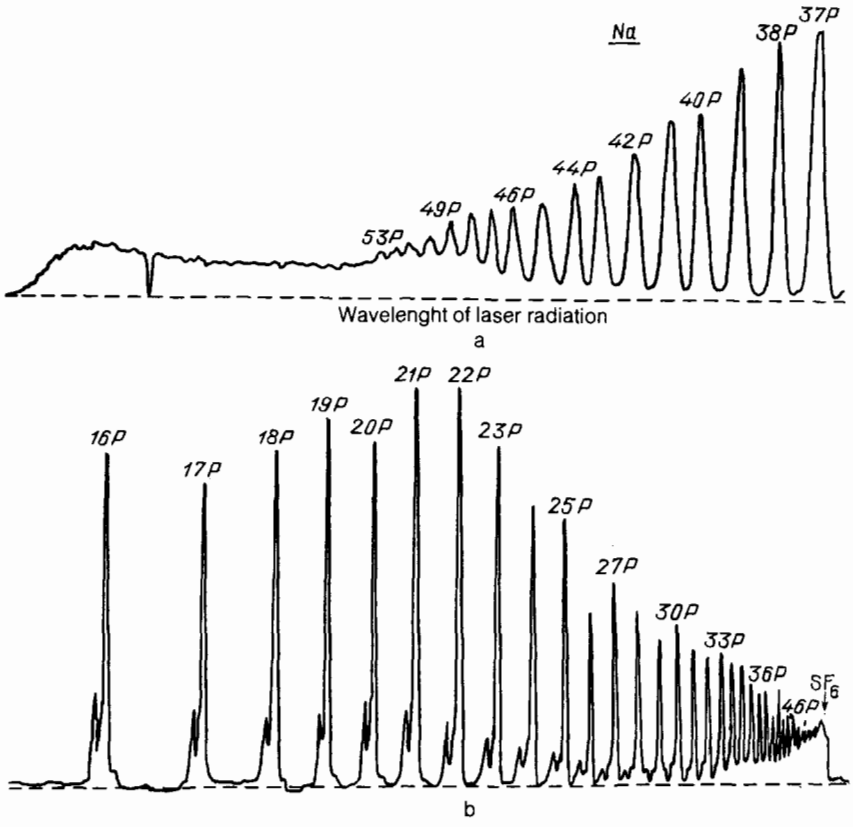

FIG. 3. Excitation spectrum of the Rydberg series of Na detected by the method of field (a) and collisional (b) ionization.[25,144]

hydrogen atoms. At the same time the transverse Doppler width, which is inversely proportional to the wavelength, also decreases.

The experimental limiting values of selectively excited Rydberg atoms of alkali elements in experiments with pulsed sources reach $n \approx 30$–50 (Refs. 30 and 31) and 60–100 (Refs. 32 and 33)—using cw dye lasers. The compensation of Doppler shifts accompanying two-photon absorption in the field of a standing wave[34,35] permits reducing significantly the transverse Doppler width of the absorption line of the atomic beam. When the ground or a metastable state is employed as the lower working state the natural width of the absorption line also decreases. As a result selective excitation using highly monochromatic sources can be driven up to $n \approx 150$–200.[36,37] Naturally, from the viewpoint of a Rydberg maser, it is difficult to expect high excitation efficiency here; a possible exception is the case of exact two-photon resonance with an intermediate state, observed, for example, in In.[38] Figure 3 shows the characteristic forms of the excitation spectra for the nP series Na,[24] recorded by the method of field and collisional ionization,[25] while Fig. 4 shows the two-photon excitation spectrum of Sr (Ref. 36) with the Doppler broadening eliminated in the field of a standing wave. At a definite value of n excitation selectivity is limited by Stark-effect broadening in the residual nonuniform electric field, since the polarizability grows as $\sim n^7$. In experiments in which special measures were taken to suppress the residual electric fields with the help of special coatings for and configurations of the metal walls screening the volume of interaction with the radiation from external fields selective excitation of Rydberg states right up to $n \approx 530$ (Ba) was achieved (Fig. 5).[147] Rydberg states have been successfully detected with the help of field ionization,[26,27] collisional ionization,[24,25] photoionization,[39] and surface ionization.[16]

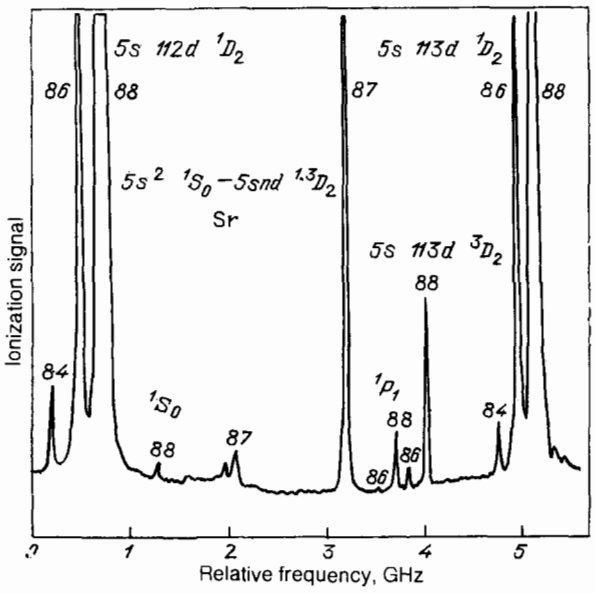

FIG. 4. Spectrum of two-photon excitation of Rydberg states of the strontium atom[36] with elimination of Doppler broadening in the field of a standing wave.

2. Rydberg states with exotic quantum numbers. Production and spectroscopy of circular states. The idea of obtaining "circular" states was proposed in Ref. 40. These are single-electron atomic states with large principal quantum number n and the maximum possible magnetic quantum number $|m| = n - 1$. Such circular states are important for experiments with Rydberg atoms in which a two-level system must be modelled. The circular state has one decay channel; this is important, for example, for observing the

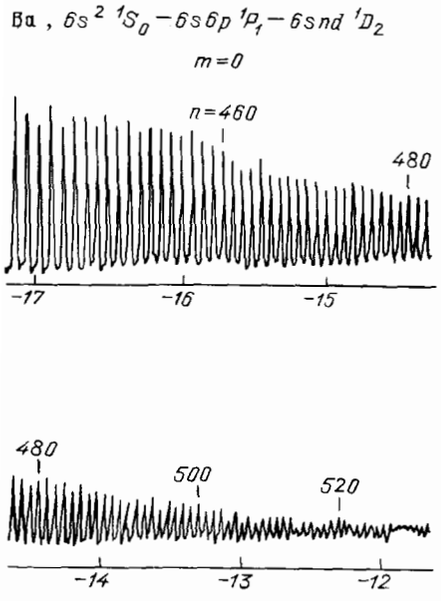

FIG. 5. The spectrum of highly excited states of the barium atom.[143] The energy is measured with respect to the ionization limit in zero field ($I = 42{,}034.902\ \text{cm}^{-1}$).

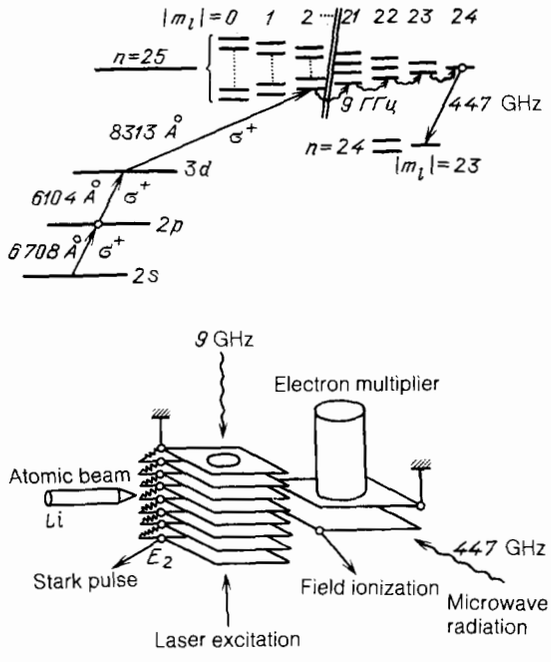

FIG. 6. Block diagram illustrating the production of circular Rydberg states of the lithium atom.[42]

suppression of spontaneous emission from a Rydberg atom by means of parallel conducting plates.[41]

Circular Rydberg states corresponding to large quantum numbers and the maximum possible projection of the orbital angular momentum on the axis of quantization are a quasiclassical atomic system with special properties. The distribution of the electron density of the outer electron in these states has the form of a thin torus with radius n^2a_0 and width na_0 (a_0 is the Bohr radius), oriented perpendicular to the axis of quantization. The center is the ionic core of the atom. Since the Rydberg electron virtually does not penetrate into the ionic core the circular states of all elements are described by the same wave functions and their binding energy differs from the hydrogen value $E_n = l^2/2a_0n^2$ by an extremely small shift $\delta E_n = -\alpha_0' e^2/2\alpha_0^4 n^8$ (α_0 is the polarizability of the ionic core). Since in this case the valence electron moves along a quasi-two-dimensional orbit the projection of the dipole moment of these states on the axis of quantization is equal to zero and therefore these states are insensitive to an electric field perpendicular to the plane of the orbit (in this direction the Stark effect is quadratic). Since there is only one channel for radiative decay (the selection rules are $\Delta n = -1$ and $\Delta m_l = -1$) the circular RSs have long spontaneous decay times, whose value increases as n^5.[139]

The method for obtaining circular Rydberg states is based on successive adiabatic transfer of excitation in a resonance microwave field[1)] and was first demonstrated by Hulet and Kleppner.[41] In one variant it is realized as follows (Fig. 6). An electron beam is passed through a stack of equidistant flat metal plates, to which uniform electric field pulses are applied (in the experiment with Li atoms performed in Ref. 42 the field intensity was equal to 200 V/cm for $n = 25$). A microwave field (9.2 GHz in Ref. 42), polarized perpendicularly to E_2 and inducing transitions between the Stark sublevels, is applied to the same plates. The direction of the electric field determines the axis of quantization of the angular momentum. For each m_l there are $n-m_l$ quasi-equidistant Stark sublevels, comprising the vertical scale of levels and denoted by parabolic quantum numbers n_1 and n_2 with $n_1 + n_2 + |m| + 1 = n$.

Three light beams, circularly polarized in the same direction (σ^+) and propagating in the direction of the electric field vector, prepare a Rydberg atom in the $n_1 = 0$ level of the sequence of the multiplet $m_l = 2$. Then the electric field E_1 is reduced adiabatically (over a time of 10 ms) from 200 V/cm to ≈ 192 V/cm, while the power (50 μW) of the microwave field at 9.2 GHz is maintained constant. As a result rapid adiabatic creation of a Rydberg atom along the sequence of microwave transitions with $\Delta m_l = +1$ occurs. Ultimately almost all Rydberg atoms are in the state $n = |m_l| - 1$. Then the atoms leave the multiplate capacitor. In working with circular states, however, the following problem arises: the external parasitic fields acting on an atom in the beam must not mix the long-lived circular state with some other state, thereby creating a preferred decay channel. In Ref. 43 this problem was solved by an elegant method, reminiscent of the method employed to stabilize a classical gyroscope. In performing experiments with states with $n = 25$ in a beam of lithium atoms Liang *et al.*[42] found that the imposition of an electric field (100–700 V/cm·μs) with a constant or slowly varying orientation perpendicular to the plane of the orbit prevents mixing of circular states with states having lower values of the angular momentum. Fields with intensity $E \sim 30$ mV/cm are sufficient to avoid mixing owing to parasitic fields with frequency $\omega_s \lesssim 1.4$ MHz ($n = 25$) without changing the transition frequency (the Stark shift is approximately 8 Hz with a transition frequency of 447 GHz). This effect is explained by the fact that the overlap integral between a circular state with a fixed axis of quantization and states with other values of n is small, and mixing by parasitic fields is prevented by artificially tying the quantization axis to a weak external field, applied, more-

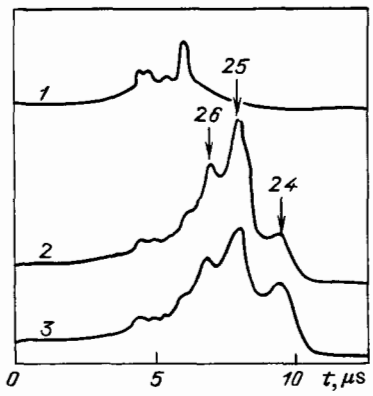

FIG. 7. The intensity of the ionization signal (arbitrary units) as a function of the scanning time. The arrows mark the signal from the corresponding level. 1—No fields with frequencies of 447 and 9 GHz;2—9 GHz switched on; 3—both microwave fields present.[42]

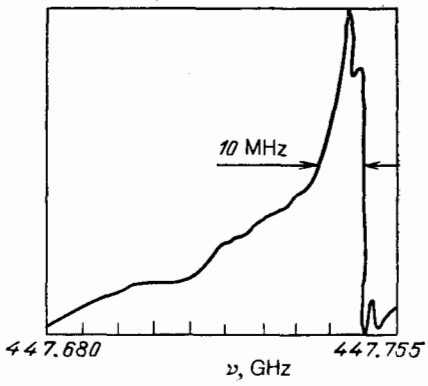

FIG. 8. Microwave resonance of circular states. The asymmetry of the spectrum is associated with the quadratic Stark effect.[42]

over, in the direction of greatest insensitivity of the orbits of the circular atom.

Figure 7 illustrates the adiabatic passage and production of circular states. A trace of the ionization signal in time under different conditions is presented. The trace 1 corresponds to the case when there is no microwave field either at 9 GHz or 447 GHz. The main peak in the signa corresponds to field ionization of a level with $n = 25$, $m_l = 2$, and $n_1 = 0$ at a moment in time when the strength of the electric field reaches 1430 V/cm, which is in good agreement with the computer calculations of the value of the critical field. The peaks in weaker fields correspond to sublevels with $m_l = 0$, 1, and 3, also excited with laser radiation. New features appear in the signal when a microwave field at 9 GHz is switched on. The largest peak, observed with 2000 V/cm, corresponds to a circular state with $n = 25$, and $m_l = 24$, while the two small peaks with 2400 kV/cm and 1730 V/cm can be ascribed to the respective levels with $n = 24$, $m_l = 23$ and $n = 26$, $m_l = 25$, 24, and 23. These neighboring levels are occupied as a result of transitions induced by thermal radiation. The computed time interval during which excitation is transferred between circular states at room temperature (~ 62.5 μs) is of the order of the transit time of the atom; this explains, in principle, the high population of levels with $n = 24$ and 26. The significant intensification of the signals 2 demonstrates the fact that the lifetime of a Rydberg atom increases when the atom is transferred into a state with high angular momentum.

Finally, the trace 3 shows the ionization signal for the case when the electric field increases linearly in time; this signal appears in the presence of a resonance microwave field at 447 GHz. One can see the change in the ratio of the amplitudes of the peaks for $n = 25$ and $n = 24$ owing to radiative transitions in a resonance field.

Microwave spectroscopy of circular states can be performed by varying the frequency of the microwave field. Figure 8 shows samples of such spectra. Strong asymmetry of resonance with a sharp dropoff on the high-frequency side and a slow (50 MHz) rise on the low-frequency side is observed. This form is characteristic for inhomogeneous broadening owing to the quadratic Stark effect. The fact that broadening arises only on the low-frequency wing of the line shows clearly that the Stark effect is quadratic, as expected for circular Rydberg states in a field oriented parallel to the quantization axis.

The position of the sharp high-frequency wing of the line permits determining the unperturbed Rydberg frequency and the Rydberg constant. In the indicated experiment[42] they turned out to be equal to $\nu_{25\text{-}24} = 447{,}749.5\ (5)$ MHz and $R = 328{,}958{,}470\ (1)\cdot 10^9$ MHz. The specially applied additional electric field made it possible to measure the quadratic Stark shift precisely $\Delta\nu = -7.11$ kHz$\cdot$(V/cm)^2.

The structure of highly excited states of atoms adsorbed on the surface of cryogenic dielectric whose dielectric constant is close to unity, for example, liquid helium $G = 1.0572$), is unusual.[86] The electronic shell of the ^{4}He atom in a highly excited state is soft, and the nucleus or ionic core of the atom fall through to the surface of the dielectric and bind with it. The helium surface is virtually impenetrable to an electron and can be described by imposing on the wave function the boundary condition $\Phi(z = 0) = 0$. The Hamiltonian of the outer electron in this case has the form

$$\hat{H} = -\frac{\hbar^2}{2m}\Delta - \frac{l^2}{r} - \frac{Ql^2}{z}, \tag{2.1}$$

where r is the distance to the nucleus, z is the distance to the helium surface, and $Q = (\epsilon - 1)/4(\epsilon + 1)$. The first term in the potential energy describes the interaction of the electron with the ionic core and the second term describes the interaction of the electron with its image. For relatively low levels of excitation the atom is in a "half-spherical" state, characterized by the quantum numbers n and l (odd) and having the energy $E_n = ml^4/2\hbar^2n^2$. The correction owing to interaction with the image is $\Delta E_n \approx a_{lm} QE_n$, where the coefficient a_{lm} increases when either index is increases. For $l = 1$ such states occur for $n < 60$. Very highly excited states belong to a different class. In this case the main interaction is the interaction of the electron with its image. The energy corresponding to such a "flat" state is given by

$$E_{K,n} = -\frac{Q^2ml^4}{2\hbar^2K^2} - \frac{ml^4}{2\hbar^2[n + (1/2)]^2}, \tag{2.2}$$

where K is the number of the levitation level and n is the principal quantum number for two-dimensional motion of the electron in the field of the nucleus. The subsequent corrections are of order $Q^{-2}(K/n)^4$ and are small for $n/K > 20$.

3. Current problems in the spectroscopy of Rydberg states. Diffusion ionization and quantum localization. A distinguishing feature of Rydberg atoms, which form the active medium of Rydberg masers, is that the coupling with the ionization continuum is strong. This coupling can sometimes be manifested in an unexpected manner in the properties of the maser. The question of the mechanism of nonlinear ionization in a microwave field is itself interesting from the viewpoint of understanding the characteristics of the excitation and decay of multilevel systems in strong fields. A discussion of the physics of this equation and a bibliography of publications up to 1983 are contained in the reviews of Refs. 18 and 45. Here we shall review the latest works.

It is well known[18] that the quasiclassical nature of highly excited states has the results that the motion of the atomic electron is stochastic. This is reflected in the appearance of the phenomenon of diffusion ionization. In the last few years the physics of this phenomenon has been studied in detail both experimentally[46–48] and theoretically.[49–57] One interesting result of the theory is that quantum-mechanical corrections partially suppress the classical chaotic motion.[51,52] Other quantum-mechanical calculations have also been performed.

The question of quantum localization has been studied from the viewpoint of "quantum mapping," i.e., the quantum-mechanical analog of the classical theory of mappings,[151] where quasienergy levels play the role of invariant tori. For one- and two-dimensional hydrogen atoms these studies have been practically completed, and their results are summarized in Refs. 152 and 153. A different approach, which is close to the strong-coupling equations in the theory of quantum localization,[154] was used in Refs. 155–157. Thus two different approaches have now been formulated for the hydrogen atom: the quantum approach, in which the stochastic instability of classical orbits, resulting in overlapping of resonances,[97] formation of a quasicontinuum, and diffusion change in the energy of the electron, is studied and the quantum approach, in which the evolution and interference of coherent wave packets and reduction of the rate of ionization are studied.[155–157] At present it is not clear how these approaches transform into one another.

Owing to the existence of a quantum defect the characteristics of multiphoton ionization of Rydberg atoms of alkali metals are in many ways different from those for the hydrogen atom.[159] For alkali metals the dominant mechanism of microwave ionization is a cascade of Landau-Zener transitions between different components of the Stark multiplets.

Among the latest experimental investigations we call attention to Ref. 46, in which microwave transitions and multiphoton ionization of highly excited hydrogen atoms with $n_l = n_1 - n_2 = -59$ polarized in an electric field were observed. With relatively low microwave powers (0.2–0.5 W) in the range 6–8 GHz resonance multiphoton transitions, owing to absorption of four to five microwave photons, were observed near the expected static-field Stark-shifted frequencies. For higher powers a smooth distribution of the obtained excited states was observed; this was regarded as confirmation of the start of "diffusion."

The most careful experiments on checking the applicability of classical dynamics to the process of multiphoton ionization of a hydrogen atom were performed recently by Koch's group.[48,158] It was shown that in a wide range of values of the parameters the ionization thresholds agree well with the classical calculations for one- and two-dimensional systems.[49,50] The observed dependence of the threshold field strength on the principal quantum number n reflected the presence of periodic orbits and surrounding island structures in the classical phase space near microwave frequencies satisfying the relation $n^3\omega = 1/4$, $1/3$, $2/5$, and $1/2$.

As regards the question of "quantum localization" as a mechanism for limiting diffusion ionization or an alternative mechanism, as a result of the interference of wave packets, experimental studies in this direction are only just beginning, and among them we call attention to the recent work on two-frequency ionization of the hydrogen atom[158] and also Ref. 164. A detailed analysis of the present situation falls outside the scope of this review.

III. THE STIMULATED EMISSION OF RYDBERG ATOMS IN A CAVITY. ONE- AND TWO-PHOTON RYDBERG MASER

Stimulated emission of Rydberg atoms in a microwave cavity is accompanied by maser generation. The physics of the generation of coherent radiation by a Rydberg maser is substantially different from what happens in the standard quantum-electronic devices– lasers and masers.

First, the spontaneous transition rates in a cavity are substantially modified owing to the fact that the density of states of the electromagnetic field in a cavity is different from that in free space. This effect is insignificant for the usual lasers and masers in view of the following facts: 1) the density of states is different from the vacuum case only in a narrow frequency band; 2) as a rule, the total number of cavity modes (longitudinal and transverse) is large; and, 3) collisions strongly affect the lifetime of the excited states. Suppression of spontaneous microwave transitions by a cavity detuned from the characteristic frequencies of the atomic transitions makes it possible to obtain extremely long atom-field interaction times.

Second, stimulated emission of an ensemble of Rydberg atoms in a cavity occurs, as a rule, in the superradiant cascade regime. The production of superradiation at optical frequencies is, one the other hand, an extremely complicated experimental problem.[138] This difference is connected both with the extremely large values of the dipole matrix elements ($d \sim n^2$ in the case of Rydberg states) and with the relative ease with which an ensemble of population-inverted atoms can be obtained in a volume whose linear dimensions are much smaller than the wavelength.

Third, the phenomenon of maser generation of two-photon transitions which are not observed in other experiments also becomes observable because the threshold for generation on a two-photon transition with existing Q-factors of superconducting microwave resonators ($Q \sim 10^{+7}$–10^9) is completely achievable. The coherent radiation obtained from such a device has even more distinct nonclassical features than the radiation of a one-photon micromaser.

On the whole, the phenomena of maser generation on Rydberg transitions are interesting in that the quantum effects which are insignificant in the usual quantum generators owing to competition with other nonlinear and nonresonance processes are especially strongly manifested on

Rydberg ensembles in rarefied atomic beams.

4. Description of experimental apparatus. Basic elements and working parameters of Rydberg masers. One-atom Rydberg maser

As any quantum generator, a maser operating on Rydberg atoms consists of a microwave cavity and an active medium (amplifier), which is a beam of excited atoms in which there is a population inversion between the Rydberg states. The experiments performed by Haroche's group, as a rule, employ an open confocal or semiconfocal cavity of the Fabry-Perot interferometer type, which forms a standing wave. This configuration has the following distinctive features.[58]

The wave vector of the microwave field is oriented along the cavity axis and can be chosen perpendicular to the direction of propagation of the atomic beam. If the beam propagates near a flat mirror, this results in a significant decrease of the Doppler width of the gain line in the microwave range as a result of the fact that the curvature of the wavefront of the microwave field is smaller.

The size of the caustic for a mode of the field of a Gaussian electromagnetic wave is determined by the relation

$$w_0 = \left(\frac{r\lambda}{2\pi}\right)^{1/2}, \tag{4.1}$$

where r is the radius of curvature of the spherical mirror. The area of the spot into which the electromagnetic field is concentrated is

$$S = \pi w_0^2 = \frac{r\lambda}{4}, \tag{4.2}$$

and it determines the saturation power. When the condition $a^2/L\lambda \gg 1$—where a is the aperture of the mirror holds—the diffraction losses are quite low and the microwave field is concentrated in the Fabry-Perot cavity. Unlike the optical range, here, when short cavities are employed, low-order longitudinal modes appear in the generation:

$$\nu_q = \frac{qc}{2L}. \tag{4.3}$$

For example, for $\nu = 75$ Gz (4 mm) and $L = 8$ mm $q = 4$. This means that there are no difficulties in selecting longitudinal modes. Since the resonator is semiconfocal $L \approx r/2$, where r is the radius of curvature of the mirror. Near the focal length the resonance condition has the following form:

$$L = \frac{\lambda}{8}(4q + m + n + 1), \tag{4.4}$$

where q, m, and n are integers. The transverse diameter of the mirror is chosen so as to increase the diffraction losses for transverse modes $m + n = 0$, but retaining the high Q-factor for longitudinal modes determined by the index q. In practice the value is equal to $a^2/r\lambda \approx 1$.

At the center of each mirror there is usually a coupling opening for injecting and extracting microwave radiation. The critical diameter of the opening is equal to about 0.3λ. Large diameters degrade the Q-factor of the cavity while small diameters degrade the transmission coefficient of the mirror for the radiation. Cooling the mirrors appreciably increases the Q-factor of the cavity, defined by the relation

$$Q = \frac{\nu_q}{\Delta\nu_p}, \tag{4.5}$$

where ν_q is the characteristic frequency of the mode and $\Delta\nu_p$ is the total width of the line.

Figure 9 shows a block diagram of a Rydberg maser. In the case of selective optical excitation of, for example, nS states a population inversion appears for the $(n-1)P$, $(n-2)P$, etc. levels. A resonance radiative transition of atoms from the nS state to lower n'P states with $n' < n$ can be induced by thermal radiation without an external microwave source. The generation process occurs when the number of atoms prepared in the upper state of the transition, which is in resonance with some mode of the cavity, for example, in the millimeter range, is sufficiently large; this process can be observed by direct detection of the microwave radiation, for example, by direct heterodyning or by measuring the density of atoms in the lower state after the Rydberg atoms have passed through the open cavity.

Generation on different transitions from a given excited state can be observed successively by smoothly adjusting the distance between the mirrors L. A large number of maser transitions was first observed in Cs (24) from 135 GHz to 1.44 GHz and in Na (17). For simplicity the field-ionization signal from the lower state is often recorded. Figure 10 shows the signals for masers starting from the $32D_{5/2}$ state of Cs. The positions of the nD states on the time scale permit identifying the levels, since the nD, $(n+1)$P, and $(n-2)$F levels are ionized at almost the same value of the field. In addition, the $(n+1)$P atoms have long lifetimes and give stronger field-ionization signals than the $(n-2)$F levels. The differences in the amplitudes and shapes of the pulses permit distinguishing the final F and P states. Figure 11 shows the ionization signals observed with excitation of the

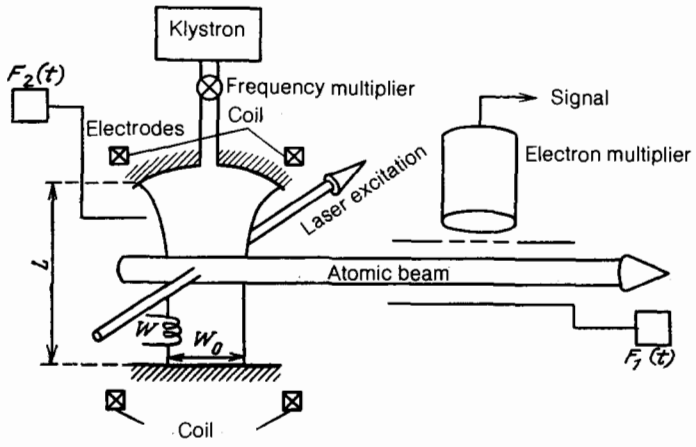

FIG. 9. Block diagram of a Rydberg maser.[58]

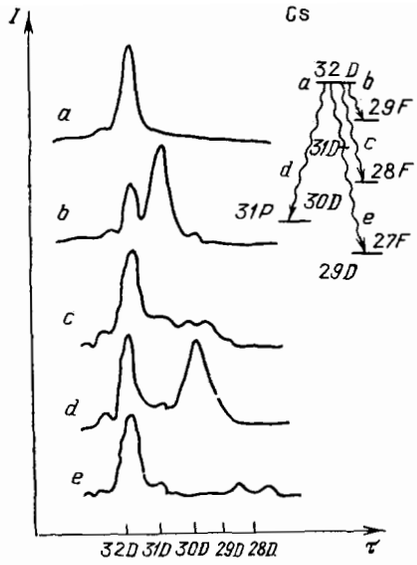

FIG. 10. Ionization signal obtained for a maser starting from the excited $32D_{5/2}$ state of Cs.[58]

30S level of Na. The $(n-1)$P and $(n-1)$D levels are ionized at the same value of the electric field. The splitting of the signal owing to the fine structure of the states permits distinguishing them from the S and D states.

A detector based on field ionization permits observing the radiation dynamics of the maser. The temporal pattern of the radiation is as follows. After some delay t_D, whose magnitude fluctuates appreciably, the maser generates a bell-shaped pulse of microwave radiation with width $3.5T_c$, where T_c is given by the relation

$$T_c^{-1} = \frac{2d^2QN^*}{\hbar\varepsilon_0 V}, \tag{4.6}$$

where d is the matrix element of the transition dipole moment, V is the effective volume of the mode, Q is the quality factor of the cavity, N^* is the number of Rydberg atoms, and ε_0 is the permittivity of the medium. It is also assumed that all atoms interact effectively with the mode of the field at an antinode. The emitted power is given by the approximate relation

$$P_{\max} \approx \frac{N^*h\nu}{3.5T_c}. \tag{4.7}$$

For example, in the experiment of Ref. 59 for the transition $33S-32P_{1/2}$ in sodium at the frequency 107892 GHz there were $3\cdot10^5$ atoms in the cavity. In this case $T_c = 50$ ns and $t_D \approx 450$ ns. The power generated should be $P_{\max} \approx 10^{-10}$ W. Taking into account the transmission of the coupling opening, the recorded power was equal to 10 pW with a pulse duration of $3.5T_c = 180$ ns.

In Ref. 59 a heterodyne detector was employed to record such a lower power level. The bandwidth of the detector (~ 14 MHz) was large enough so that short microwave pulses were not broadened too much. A backward wave tube, whose generation frequency was locked to the frequency of a klystron with quartz stabilization, was employed as the heterodyne generator. The intermediate frequency was equal to 130 MHz.

A beam of rubidium Rydberg atoms was employed for realizing experimentally a one-atom maser (Fig. 12).[1-3] The microwave cavity was carefully screened from the beam source with copper plates, which were cooled with water, liquid nitrogen, and liquid helium. The Rydberg states of the rubidium atom were selectively populated with the help of the second harmonic of cw ring dye laser and the atoms entered the liquid-helium-cooled cavity. The atoms passing through the cavity were detected by the method of field ionization. The electrons were detected with a channel multiplier. The transition of atoms from the initially prepared state into the lower state was detected as a drop in the electron counting rate.

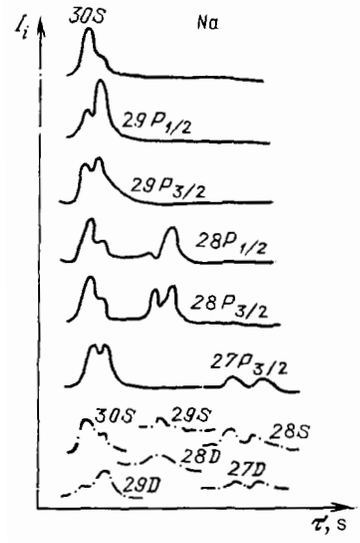

FIG. 11. Ionization signals obtained for a maser starting from the 30S state of sodium.[58]

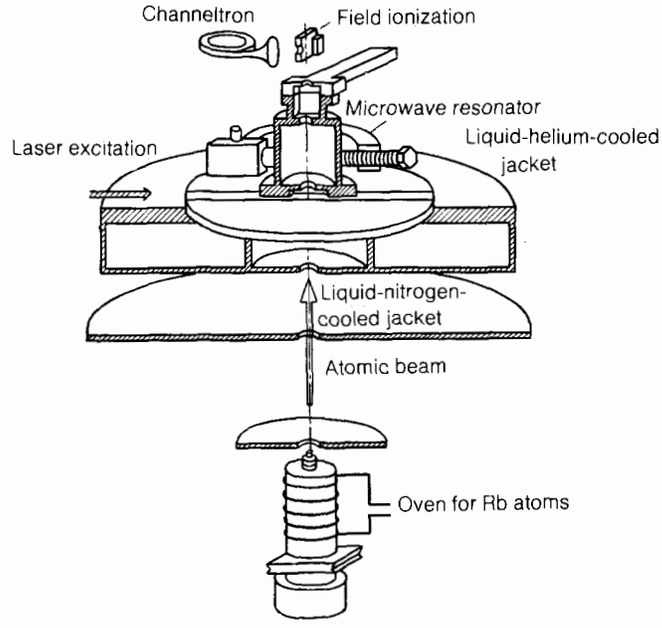

FIG. 12. Experimental diagram of a one-atom Rydberg maser realized in Ref. 1.

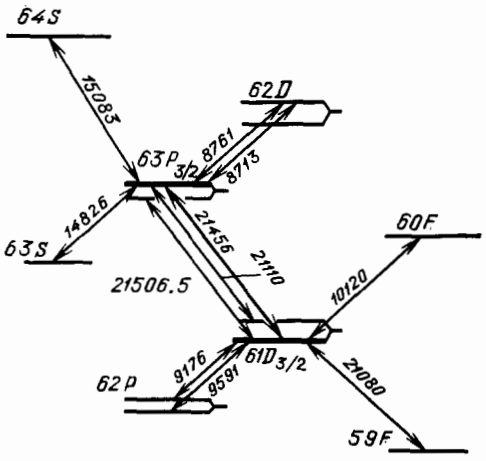

FIG. 13. The typical working scheme of levels of the Rydberg maser operating on highly excited states of the ^{85}Rb atom. The working transitions are $63P_{3/2} \rightarrow 61D_{3/2}$ and $63P_{3/2} \rightarrow 61D_{5/2}$.

The microwave cylindrical cavity (24.8 mm in diameter and 24 mm long) was made of pure Nb. The temperature of the cavity was varied from 4.3 to 2.0 K and the Q-factor varied correspondingly from $1.7 \cdot 10^7$ up to $8 \cdot 10^8$. The atomic beam passed through the cylindrical cavity along its axis, so that only the TE_{1np} and TM_{1np} modes had a nonvanishing transverse electric field. The TE_{121} mode was employed in the experiments. The electric field of this mode is linearly polarized and forms a half-wave along the cavity axis. In an ideal cylindrical cavity it is doubly degenerate. The degeneracy was eliminated by slightly deforming the circular cross section into an oval; this determined the direction of polarization of the field. A piezoelectric ceramic was employed for fine tuning (0.5 MHz/1500 V). A diagram of the working levels of the Rydberg maser is shown in Fig. 13. The working transition was $63P_{3/2} \rightarrow 61D_{5/2}$ of the rubidium isotope ^{85}Rb. Since the fine splitting of the upper state was equal to 396 MHz narrow-band UV radiation ($\Delta\nu \sim 2$MHz) permitted excitation of only one sublevel of the fine structure

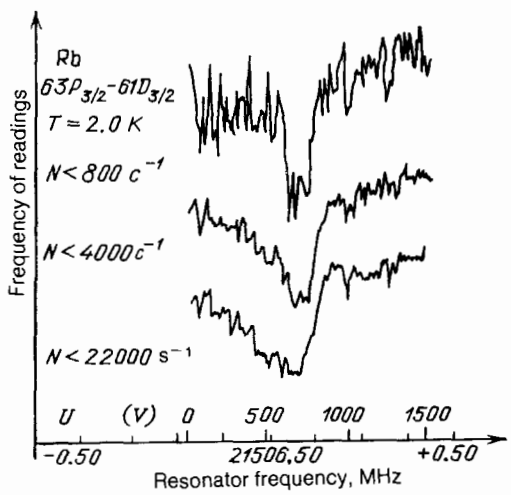

FIG. 14. Resonances of the maser at $T = 2$ K for different atomic flow rates in the cavity.[1]

of the $63P_{3/2}$ state. To obtain maser generation the cavity was tuned to the frequency of the transition $63P_{3/2} \rightarrow 61D_{3/2}$ (21.50658 GHz).

At a cavity temperature of 2 K a decrease in the density of atoms in the $63P_{3/2}$ state was observed with atomic flows of 800 atoms/s. Increasing the flow resulted in field-induced broadening of the signal, followed by symmetry and shift (Fig. 14). This shift was caused by the dynamic Stark effect owing to the closeness (~ 50 MHz) of the transition $63P_{3/2} \rightarrow 61D_{5/2}$. The observed broadening of the signal indicates that photons are repeatedly exchanged between the Rydberg atoms and the cavity field.

If the average passage time of the Rydberg atoms through the cavity ($\sim 80\,\mu$s) and the magnitude of the flow (~ 800 atoms/s) are taken into account, it is found that on the average 0.06 Rydberg atoms are present in the cavity. According to Poisson statistics this means that 99% of the events are due to single atoms. This clearly shows that one Rydberg atom can maintain steady-state generation. Since the microwave transition saturates, half of the initially excited atoms leave the cavity in the lower $61D_{3/2}$ state. Decay into other states can be neglected over the average passage time of $\sim 80\,\mu$s at $T = 2$K. The energy emitted by these atoms is stored in the cavity over the period of time during which the field in the cavity decays and thereby increases the field strength. The average number of photons left in the cavity by the Rydberg atoms is given by the relation $\bar{n}_m = T_c N^*/2$, where T_c is the characteristic decay time of the field in the cavity and N^* is the number of Rydberg atoms entering the cavity per unit time. With a maximum particle flow of $N^* = 22 \cdot 10^3$ atoms/s, $\bar{n}_m = 55$ photons at 2 K ($T_r = 5\,\mu$s) and $\bar{n}_m = 1.4$ photons at 4.3 K ($T_c = 0.13\,\mu$s). The latter value is much less than the average number of thermal photons $\bar{n}_T = 4$ at 4.3 K. For $N^* = 800$ atoms/s $\bar{n}_m = 2$ at 2 K. This meant that the energy of the radiation generated by the Rydberg atoms was the same as that of the thermal radiation ($\bar{n}_T = 1.5$).

The velocity (time-of-flight) spread of the atoms does not permit observing directly the Rabi nutation and checking the dynamics of the interaction of a single atom with one cavity mode. In Ref. 3 a multislit Fizeau selector was employed to obtain a monoenergetic beam of atoms. This velocity selector consisted of nine disks rotating with the same velocity. Each disk had 1486 radial slits (their width and spacing equalled 0.2 mm). The width of the velocity distribution of the atoms was equal to about 4%. This made it possible to observe experimentally a number of effects which comprise a check of the quantum theory of masers.[1-3]

The interaction of the cavity field with an atom is usually described with the help of an exactly solvable model, which was introduced in 1963 by Jaynes and Cummings[11,85] to describe the interaction of a two-level quantum system with one cavity mode. The atoms in the cavity are described by three Pauli operators $\hat{\sigma}_\pm$ and $\hat{\sigma}_3$ while the field is described by the boson operators $\hat{a}_\lambda$ and $\hat{a}_\lambda^+$ which satisfy the commutation relations

$$[\hat{\sigma}_3, \hat{\sigma}_\pm] = \mp \hat{\sigma}_\pm, \quad [\hat{\sigma}_+, \hat{\sigma}_-] = \sigma_3, \quad [\hat{a}_\lambda, \hat{a}_\lambda^+] = \delta_{\lambda\lambda'}. \quad (4.8)$$

The electromagnetic field in the cavity is described by the expressions

$$\mathbf{E} = -\sum (2\pi\hbar\omega_\lambda)^{1/2} (\hat{a}_\lambda + \hat{a}_\lambda^+)\, \mathbf{E}_\lambda(\mathbf{r}),$$

$$\mathbf{H} = \sum \left(\frac{2\pi\hbar}{\omega_\lambda}\right)^{1/2} (\hat{a}_\lambda - \hat{a}_\lambda^+)\, \mathbf{H}_\lambda(\mathbf{r}), \qquad (4.9)$$

where $\mathbf{E}_\lambda(\mathbf{r})$ and $\mathbf{H}_\lambda(\mathbf{r})$ are the characteristic modes of the cavity. The Hamiltonian of the model has the form

$$\hat{H} = \frac{\hbar\omega_0}{2}\hat{\sigma}_3 + \hbar\omega_p\left(\hat{a}_\lambda\hat{a}_\lambda^+ + \frac{1}{2}\right) + \hbar\lambda(\hat{\sigma}_+\hat{a}_\lambda + \hat{a}_\lambda^+\hat{\sigma}_-), \qquad (4.10)$$

where ω_0 is the frequency of the atomic transition, ω_c is the characteristic frequency of the cavity, and λ is the Rabi frequency of one photon,

$$\lambda = \left(\frac{\pi e^2\omega_p}{mV_c\omega_0}\right)^{1/2}.$$

The first term in Eq. (4.10) describes the characteristic energy of the atom, the second term describes the characteristic energy of the field, and the third term describes the dipole interaction of the atom and the field in the rotating-wave approximation. The interaction Hamiltonian has two types of matrix elements—"resonance" elements corresponding to the transition of the atom into an excited state on absorption of a photon and "off-resonance" elements corresponding to the coupling of states with $(E_2 - E_1 + \hbar\omega) \sim 2\hbar\omega$ with a simultaneous change in the occupation numbers. The problem of generation in a Rydberg maser is naturally formulated in terms of the problem of passage of one (or an ensemble) of two-level atoms through the cavity. Jaynes and Cummings studied two types of initial conditions: a coherent state and a chaotic field of thermal radiation.[11,85]

If in the initial state the atom is excited, then the following expressions describing the coherent state can be derived for the correlation functions of the field which are determined for the positive and negative components of the field E^+ and E^-:

$$\langle E^-\rangle_c(t) = -\frac{2\lambda}{d}\, e^{i\omega t} S_2(\bar{n}, t),$$

$$\langle E^-E^+\rangle_c(t) = \left(\frac{2\lambda}{d}\right)^2 (\bar{n} + S_1(\bar{n}, \lambda t)). \qquad (4.11)$$

Here $\bar{d}$ is the average dipole moment of the atom and S_1 and S_1 are determined by the expressions

$$S_1(\bar{n}, \lambda t) = \sum_{\bar{n}=0}^{\infty} \frac{e^{-\bar{n}}\bar{n}^{\bar{n}}}{\bar{n}!} \sin^2[(\bar{n}+1)^{1/2}\lambda t],$$

$$S_2(\bar{n}, \lambda t) = \sum_{\bar{n}=0}^{\infty} \{\cos[(\bar{n}+1)^{1/2}\lambda t]\cos[(\bar{n}+2)^{1/2}\lambda t] + \left(\frac{\bar{n}+2}{\bar{n}+1}\right)^{1/2} \sin[(\bar{n}+1)^{1/2}\lambda t]\sin[(\bar{n}+2)^{1/2}\lambda t]\}\frac{e^{-\bar{n}}\bar{n}^{\bar{n}}}{\bar{n}!}. \qquad (4.12)$$

This solution essentially represents only one physical effect—Rabi oscillation induced by the field of n photons (Fig. 15). The amplitudes for the atoms and fields are obtained by summing over the corresponding probability distributions. This is understandable, since the present model contains only two parameters—the Rabi frequency of one photon and the detuning. The introduction of decay into the cavity mode substantially modifies the formalism of the model.[90] The

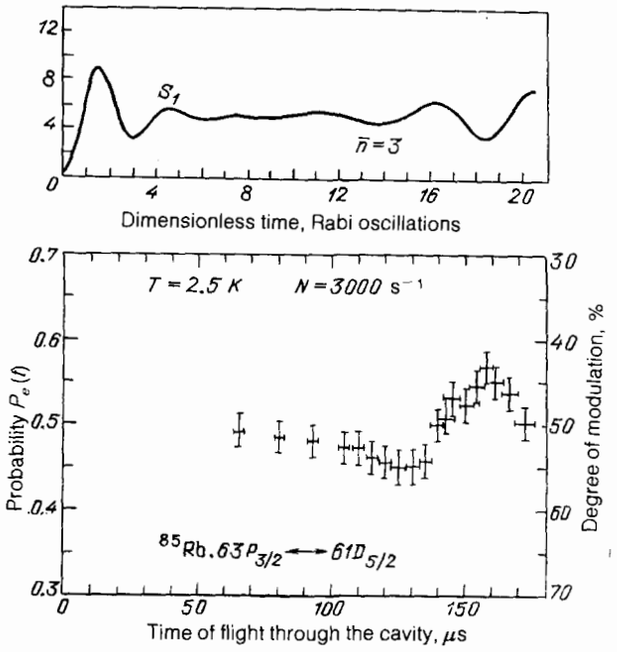

FIG. 15. The measured probability of detecting atoms in the upper working level of the maser $63P_{3/2}$ in a cavity tuned to the transition $63P_{3/2} - 61D_{5/2}$ of the rubidium atom. The flow of atoms $N = 3000\,s^{-1}$.

expression for S_1 given in Eq. (4.12) incorporates the so-called "Cummings collapse"—nondissipative decay of the correlation at a rate $\sim(\lambda t)^2/2$, which is independent of the parameters of the atom as well as the frequency ω_c of the cavity is equal to the Rabi frequency of one photon in the cavity, and is expressed by the purely classical quantity λ but with a nonexponential decay law. This surprising phenomenon is explained by the fact that in a field with an uncertain number of photons the Bloch vector undergoes diffusion over the unit sphere as a result of the impulses of separate photons. In the course of this diffusion the "memory" of the starting value of the correlation functions is lost. However the phase information in an infinite-Q cavity is preserved and the quantum correlations are partially restored. This is the so-called "Eberly revival,"[87-94] which was observed in experiments with a one-atom Rydberg maser (Fig. 15b).[3] The physical meaning of "revival" is that n-photon oscillations of the field can once again be partially synchronized after a certain time interval. This is a purely quantum effect, since its parameters, for example, the time $T_m = 4\pi n^{1/2} m/\lambda\,(m = 0 \pm 1 \ldots)$, are related explicitly with the total average number of photons in the cavity $\bar{n}$.

One of the most important characteristics of a Rydberg maser is the fundamental possibility of measuring the statistics of photons during the generation process. The establishment of the fact that it is of a non-Poisson character in a number of cases[3,109] was a striking confirmation of the results of nonperturbative quantum electrodynamics.[87-89]

In this review we discussed very briefly the quantum electrodynamics of a microwave field, i.e., the region where the quantum properties of the electromagnetic radiation itself are important for understanding the dynamics of a Rydberg maser. There is an extensive literature on this subject.

References 96–100 are devoted to the different dynamic regimes of the "atom + cavity" system. In the course of evo-

lution the photon field in a Rydberg maser can acquire a nonclassical statistics—it can transform into a compressed state.[101,102] Questions pertaining to the nonclassical statistics of the electromagnetic field in a cavity are elucidated in Refs. 103–106, 137, 140, 141, 148, and 149.

The quantum theory of Rydberg masers and the closely related different generalizations of the Jaynes-Cummings model are further developed in Refs. 107–109, 111–119, 133, 135, and 150. The most interesting results here are the "radiation trapping,"[107–109] multistable regimes in a Rydberg maser,[117] and the discovery of supersymmetry[126–131,134] in the Jaynes-Cummings model[150] and its relation with the Rabi vacuum splitting[89]—the splitting of the ground state of a two-level system by the field of quantum fluctuations.

A fundamental result which follows from the quantum dynamics of rarefied beam of population-inverted atoms[95] is that the field in the cavity transforms from a chaotic thermal field through a coherent field into a Fok or n-photon state of the electromagnetic field,[147] i.e. into a state in which there are no fluctuations of the number of photons. The experiments performed by H. Walther's group, having achieved a quality factor of the microwave cavity $Q\sim 2\cdot 10^{11}$ at frequencies $\omega/2\pi\sim 20$ GHz, are now at the threshold of reliable detection of the Fok state.

5. Two-photon micromaser. Classical model. Quantum theory. Pulsations and chaos. Experimental realization. The theory of a two-photon Rydberg maser was developed in Ref. 115. Unlike the proposed[120–122] two-photon laser, which is very difficult to realize in practice owing to the extremely low gain and competing nonlinear processes (nonlinear shift, Raman scattering), owing to its much lower generation thresholds the two-photon Rydberg micromaser promises to be realizable in practice.

An important distinction of a two-photon micromaser is the Rabi precession with the "two-photon Rabi frequency," proportional not to the strength of the electric field but rather to its intensity:

$$\Omega_{ef}(\bar{N})=\frac{\Omega_{el}\Omega_{lf}\bar{N}}{\Delta}. \tag{5.1}$$

Two-photon Rabi oscillations were first observed recently in Kleppner's group at MIT.[163] In the experiments the 52P–51P transition in the calcium atom and a pulsed microwave field with a frequency of 35 GHz were employed. The form of the oscillations is shown in Fig. 16. The temperature of the superconducting cavity was $T=2$ K and the Q-factor exceeded 10^7. The first direct observation of the two-photon dynamic Stark effect and measurement of the two-photon Rabi frequency were made at the Institute of Thermal Physics of the Siberian Branch of the Academy of Sciences in Rydberg Na atoms, which were studied by the method of three-level two-photon microwave spectroscopy.[146] Figure 17 shows a picture of this effect.

If the atom is prepared in the state $|e>$, then the probability of finding it in this state is equal to

$$P_e(t)\approx 1-\sin^2(\Omega_{ef}(\bar{N})t)=\frac{1}{2}(1+\cos(\Omega(\bar{N})t)),$$
$$\Omega(\bar{N})=2\Omega_{el}\Omega_{lf}\bar{N}\Delta^{-1}. \tag{5.2}$$

The theory of the two-photon micromaser[115] is actually based on a description on the basis of the method of "dressed atoms,"[123,125] since the dynamic Stark shift, which appears in the same order of perturbation theory, must be taken into account together with the two-photon Rabi precession. The numerical value of the two-photon Rabi frequency with one photon in the cavity mode is 4000 s^{-1} with $\langle e|d|i\rangle$, $\langle e|d|f\rangle = 1.5\cdot 10^3 ea_0$ for $\Omega(\bar{N}=1)$.

An expression for the generation threshold can be obtained quite simply from the conditions $t_c \gg t_{at}, \tau_{int}$:

$$\bar{N}\approx\frac{2t_c}{t_{at}},\quad \Omega(\bar{N})\tau_{int}=\Omega(1)\frac{2t_c}{t_{at}}\tau_{int}\sim 1, \tag{5.3}$$

where τ_{int} is the passage time of the atom through the resonator, t_{at} is the average time between the "injections" of atoms, and $\Omega(\bar{N})\tau_{int}\sim\pi$ is the condition that the atom exchanged with a mode of the field is a significant part of the electromagnetic energy. We have

$$t_{at}^{-1}=\frac{\Omega}{2\Omega(1)\tau_{Int}t_c},\quad \bar{N}=\frac{2t_p}{t_{at}}=\frac{\pi}{\Omega(1)\tau_{int}}; \tag{5.4}$$

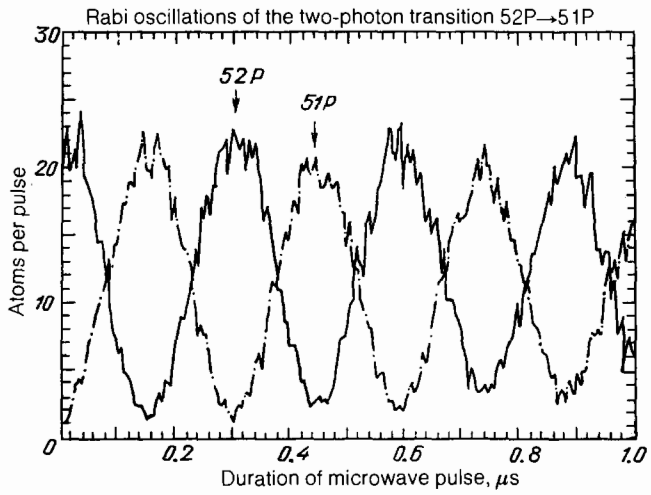

FIG. 16. Two-photon Rabi oscillations observed on the transition 52P-51P of the calcium atom in a pulsed 35 GHz microwave field.[162]

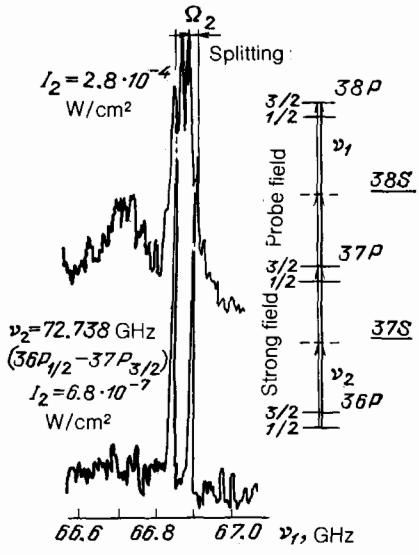

FIG. 17. Two-photon dynamic Stark effect observed with three-level microwave spectroscopy of the Rydberg 36P sodium atom.[146]

in the quasiclassical approximation the kinetic equation describing generation for an average number of photons in a mode has the same form as in Ref. 115.

Such an equation, characteristic for generation of multistable devices, shows that the response of a micromaser is complicated, the limit cycle could be modified by blackbody radiation noise, the photon statistics could be nonclassical, etc.[142]

It is possible to derive a more accurate kinetic equation[115] for the function

$$P_N(t) = \sum_{N'} NP_{NN'},$$

which denotes the probability of finding the number of photons in a mode as a function of time; this equation permits calculating the variance of the number of photons and establishing that the two-photon micromaser, starting from a Poisson field, monotonically reprocesses it into a field with sub-Poisson variance. The computed characteristic in this case is the variance of the number of photons ΔN: $\pi(N,t) = P_e^N(t)$,

$$\Delta N = \frac{(\langle N^2\rangle - \langle N\rangle^2)^{1/2}}{\langle N^2\rangle^{1/2}} = \left[\sum_N \frac{(N^2 - \bar{N}^2)\,\pi\,(N_{\text{at}})}{\bar{N}\,(N_{\text{at}})}\right]^{1/2}. \quad (5.5)$$

The following expression can be derived for the probability sought:

$$P_e^N(t) = 1 - \frac{2\Omega_{\text{li}}^2\Omega_{\text{if}}^2\,(N+1)\,(N+2)}{\Delta^2\Omega^2\,(N)}\,(1 - \cos\Omega\,(N)\,t). \quad (5.6)$$

The formula (5.6), together with (5.5) and (5.3), completely describes the single-photon statistics of the process of generation in a two-photon micromaser.

The theory of generation in a two-photon micromaser[115] is patterned after the theory of the generation in a one-photon Rydberg maser and is based on reducing the system of "dressed" states for the three-level system to the "dressed" two-level system. The method of the Fokker-Planck equation, proposed in Ref. 12, for the numbers of photons makes it possible to analyze the problem quite completely. Making the substitution $n = M/2N_{\text{ex}}$ and $\delta = 1/2N_{\text{ex}}$ and making the assumption that the pumping rate is high enough (this also corresponds to large numbers of photons in the cavity), we obtain

$$\begin{aligned}\frac{\partial}{\partial\tau}\rho(n,\tau) &= -\rho(n,\tau)\left(1 - \int_0^\infty d\varphi_{\text{int}}\widetilde{P}(\varphi_{\text{int}})\,|\,\widetilde{A}(n,\varphi_{\text{int}})\,|^2\right)\\ &+ \rho(n-2\delta,\tau)\left(1 - \int_0^\infty d\varphi_{\text{int}}\widetilde{P}(\varphi_{\text{int}})\,|\,\widetilde{A}(n-2\delta\varphi_{\text{int}})\,|^2\right)\\ &- 2\,[n + N_T(2n+\delta)]\,\rho(n,\tau)\\ &+ 2\,(N_T+1)\,(n+\delta)\,\rho(n+\delta,\tau)\\ &+ 2N_T n\rho((n-\delta),\tau),\end{aligned} \quad (5.7)$$

N_T is the number of blackbody photons, $\tau = Rt$, and $n_T = \delta N_T$, where we introduced for generality the distribution of atoms over the times of flight $P(\varphi_{\text{int}})$, $\varphi_{\text{int}} = R\tau_{\text{int}}$. The effect of the spread over the times of flight (the nonmonochromatic nature of the atomic beam) reduces approximately to the following: for the Gaussian function

$$\widetilde{P}(\varphi_{\text{int}}) = (2\pi\sigma)^{-1/2}\exp\left[\frac{-(\varphi-\varphi_{\text{int}})^2}{2\sigma^2}\right]$$

an equation can be derived for the average number of photons $\bar{n} = (1/2N_{ex})\times\Sigma_N N\rho_{NN}$:

$$\bar{n} - n_T = \frac{1}{2}\,[1 - e^{-2\sigma^2\bar{n}-\delta}\cos(2\bar{n}\varphi_{\text{int}})]. \quad (5.8)$$

We can see that the effect of the nonmonochromaticity of the beam reduces to suppression of the interference structure induced in the n-particle amplitudes by Rabi oscillations.

The dynamics of the two-photon Rydberg maser, like, by the way, that of the single-photon maser also, can be traced based on equations of the Fokker-Planck type:

$$\begin{aligned}&\frac{\partial}{\partial\tau}\rho(n,\tau) = -\delta\frac{\partial}{\partial n}(a_1(n)\,\rho(n,\tau)) + \frac{\delta^2}{2}\frac{\partial^2}{\partial n^2}(a_2(n)\,\rho(n,\tau)),\\ &a_1(n) = 2\int_0^\infty d\varphi_{\text{int}}\widetilde{P}(\varphi_{\text{int}})\left[\sin^2(n\varphi_{\text{int}}) + \frac{3\delta}{2}\sin(2n\varphi_{\text{int}}) - (n-n_T)\right],\\ &a_2(n) = 4\int_0^\infty d\varphi_{\text{int}}\widetilde{P}(\varphi_{\text{int}})\sin^2(n\varphi_{\text{int}}) + 2n\,(N_T+1),\end{aligned} \quad (5.9)$$

and the expansion parameter δ plays the role of a quasiclassicity parameter.

Here the "slow" process, determining the applicability of the Fokker-Planck equation, is the change in the atomic population and the average phase of the field as compared with the "fast" frequency of Rabi oscillations in a field with a quite large number of quanta.

The stationary state of a micromaser is described by the "Boltzmann distribution"

$$\begin{aligned}&P^S(n) = \exp\left(-\frac{2V_F(n)}{\delta}\right),\\ &V_F = -\int_0^n \frac{a_1(n')}{a_2(n')}\,dn' + \frac{\delta}{2}\ln a_2(n) - \frac{\delta}{2}\ln c.\end{aligned} \quad (5.10)$$

The effective potential $V_F(n)$ is virtually independent of δ and it can have several minima (Fig. 18), depending on the value of φ_{int}; this is a clear indication of multistability and hysteretic behavior.

The equations (5.5) and (5.7) can be employed to determine the sub-Poisson statistics of the photons. Figure 19 shows the quantity $\Delta N = \delta N(\varphi_{\text{int}})$. The peak of the distribution ΔN, where the fluctuations in the number of particles is large, apparently corresponds to the transition of the micromaser through the generation threshold and establishment of a phase-coherent state. The remarkable properties of a two-photon Rydberg maser with respect to the reproducibility of the states of a field with nonclassical statistics are an intriguing direction for further experimental studies.

An experiment with rubidium (^{85}Rb) on the transition $40S_{1/2}$–$39S_{1/2}$ was successfully performed at the École Normal at the University of Paris.[9] This was the first realization of a two-photon quantum generator, in which a population-

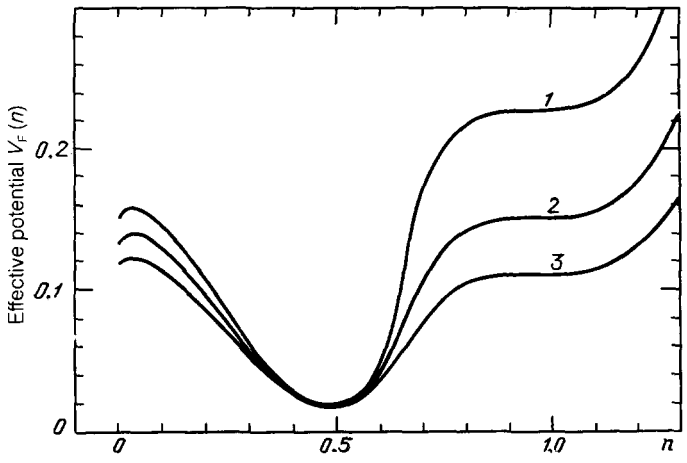

FIG. 18. The effective potential $V_{F(n)}$ for $\varphi_{int} = 0.9(1)$, $\varphi_{int} = 1.5$ (2), and $\varphi_{int} = 5/2$ (3).

inverted atomic medium emitted into a cavity tuned to the frequency of a two-photon transition. The success of the experiment is determined by two factors. The gain on two-photon transitions is usually extremely small, and the realization of a two-photon laser or maser requires extremely large densities of excited atoms, when undesirable competing effects could dominate (multiwave mixing, collisional quenching, collision broadening, and SRS). In the microwave range it is possible to achieve, using superconducting materials, record high values of the quality-factor of the cavity ($Q \sim 10^8$–10^9) and therefore to reduce markedly the gain requirements. Aside from giant dipole moments alkali-metal Rydberg atoms have an additional property which increases by many orders of magnitude the cross section for two-photon amplification in a Rydberg maser. The point is that because of the specific values of the quantum defects for the S and P series, in using S–S transitions the P states lie almost midway between the S–S states with a relative accuracy, for example, of about $5 \cdot 10^{-4}$ for $n = 40$ in ^{85}Rb. Figure 20a shows the level diagram of a two-photon Rydberg maser, realized in Ref. 9, the values of the frequencies, and the detunings from intermediate resonance. A four-step process ($5S_{1/2} \rightarrow 5P_{3/2} \rightarrow 6S_{5/2} \rightarrow 40P_{3/2} \rightarrow 40S_{1/2}$) was employed to excite ^{85}Rb into the $40S_{1/2}$ state. The required wavelengths $\lambda_1 = 7802$ Å, $\lambda_2 = 7759$ Å, and $\lambda_3 = 1.2644$ were obtained in the first three steps with the help of single-frequency semiconductor cw heterolasers, and the upper working state was prepared by means of an induced transition in a microwave field at a frequency of 62 GHz. Special measures were taken to ensure that the radiation obtained from an X-band stabilized klystron with multiplication with the help of a harmonics generator would be reflected from the input into the maser cavity. As a result, only excited atoms, whose flow rate equalled $6 \cdot 10^7$ atoms/sec, entered the liquid-helium cooled niobium cavity (7.5 mm long and 7.7 mm in diameter), tuned to the TE_{21} mode. This cavity was fabricated at CERN and its Q factor $\sim 10^8$ at $T = 1.7$ K and $Q = 3 \cdot 10^7$ at $T = 2.5$ K. Since the number of thermal photons in a mode with $T = 1.7$ K was ~ 0.17 the thermal radiation can be neglected.

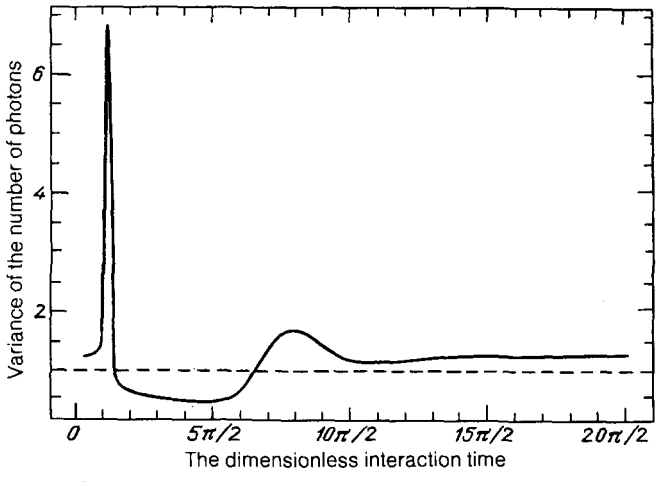

FIG. 19. The theoretical prediction[115] of sub-Poisson statistics of the generation of a two-photon micromaser: variance of the average number of photons as a function of φ_{int}. The dynamics of the distribution of the number of photons for $\varphi_{int} = 5/2$, $N_T = 0$, and $N_{ex} = 30$. The starting distribution is a coherent state with $\langle N \rangle = 45$.

Because of the closeness of the one-photon transition on which maser generation could be easily achieved the precise tuning of the cavity on the two-photon transition was the critical point of the experiment. For this reason, Brune *et al.*[9] determined the frequency of the cavity to an within $\pm$ 10 kHz in special experiments on Doppler-free two-photon spectroscopy. Precise tuning of the cavity to the two-photon transition frequency was achieved in the experiment by mechanical deformation of the walls of the niobium superconducting cavity (Fig. 20b); at liquid-helium temperatures such deformations are elastic, ensuring that the frequency tuning is reversible.

Since it was difficult to detect directly the microwave radiation of the maser the generation was detected by observing the sharp change in the populations of the $40S_{1/2}$ and $39S_{1/2}$ levels. The density of Rydberg atoms which leave the superconducting cavity in these states was measured by the method of field ionization with a 7 kHz electric field with a triangular pulse shape. The time behavior of the atomic populations is shown in Fig. 21. As the flow of atoms is intensified a sharp change in the form of the signal (*a* and *b*) was recorded at a definite moment in time; this change was interpreted as resulting from the achievement of the generation threshold of the two-photon maser. An abrupt occupation of

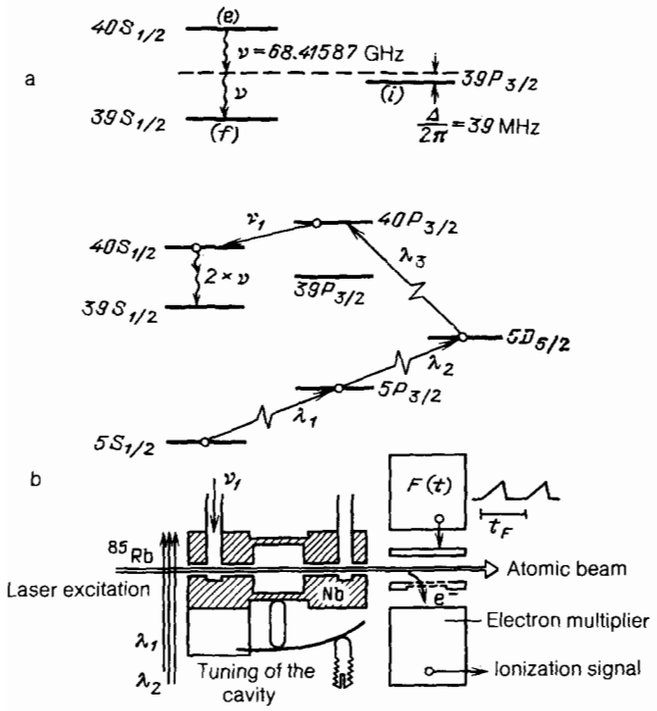

FIG. 20. Diagram of levels in a two-photon micromaser (a) and experimental diagram of a two-photon Rydberg maser (b).[9]

the $39S_{1/2}$ state occurred with an atomic flow of $(2 \pm 1) \cdot 10^5$ atoms/sec, and this value agreed satisfactorily with the threshold predicted by the authors. The dependence of the signal on the frequency of the cavity (Fig. 22) indicates a narrow gain line. It is significant that the region of restructuring (~ 50 kHz) corresponds to the independently measured frequency of the two-photon transition and is three orders of magnitude smaller than the frequency detuning from the 40S–39P one-photon transition. To eliminate the possibility of a one-photon generation cascade $40S_{1/2} - 39P_{3/2} - 39S_{1/2}$, Brune *et al.*[9] checked the density of atoms in the intermediate $39P_{3/2}$ state. Since this level ionizes practically in the same field as does the $40S_{1/2}$ state it cannot be detected directly. For this reason the beam of passing Rydberg atoms was irradiated with a microwave field at the frequency of the transition $39P_{3/2} - 37D_{5/2}$ (99.5 GHz) below the maser cavity and it was found that the ionization signal accompanying maser generation did not change. This indicated that the $39P_{3/2}$ level is not occupied in the process of generation, i.e., there is no one-photon cascade.

An interesting effect, which is being researched, is the delay in generation, which under certain conditions is significant, when above-threshold pumping of the maser is switched on suddenly. The frequency shifts owing to the dynamic Stark effect of the two-photon transition, hysteresis, multistable behavior, and statistical fluctuations are also under study. It should be pointed out that the power of the two-photon Rydberg maser radiation in the cavity is 10^{-18}–$2 \cdot 10^{17}$ W. Direct detection of this very weak microwave signal would provide extremely interesting information.

The properties of the two-photon maser must, of course, be studied in detail. Thus the width of the gain line, presented in Fig. 22, of a two-photon maser at half-height is 30 kHz, which is realized only if the Doppler shifts are compensated in the medium because of a close-lying strong (~ 1500 a.u.) allowed one-photon transition, can also be observed, especially with a lower cavity Q-factor. The role of weak residual electric fields is unclear. The first experimen-

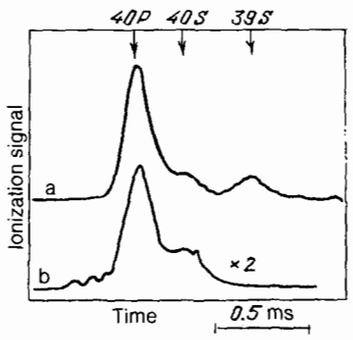

FIG. 21. The atomic populations in a two-photon Rydberg maser as a function of time.[9]

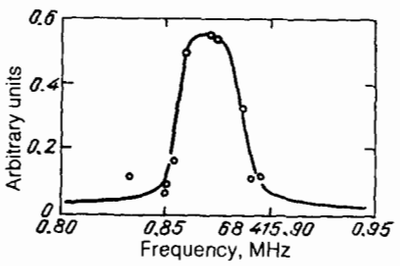

FIG. 22. The signal of a two-photon maser as a function of the cavity frequency.[9]

tal realization of a two-photon Rydberg maser nonetheless opens up a completely new direction of research.

IV. RADIATION EFFECTS IN THE SPONTANEOUS AND INDUCED EMISSION FROM RYDBERG ATOMS

6. Separation of the contribution of induced processes. Modification of the spontaneous emission in a cavity. An interesting physical effect is the modification of spontaneous emission by an external cavity. Spontaneous emission is usually regarded as an unavoidable consequence of the coupling between matter and the vacuum. However by surrounding an atom with a cavity in which there are no modes at the transition frequency the spontaneous emission can be suppressed or "switched off."

Indeed the photon density of states in a cavity differs from that in free space. In the case when the quality factor of the cavity is quite small (the decay time of the field is less than the inverse Rabi frequency) the probability of spontaneous emission is simply renormalized to the new density of states.[10,61] This fact was first noticed by Purcell, who pointed out that if the cavity is tuned to the frequency of an atomic transition spontaneous emission occurs

$$f_c = \frac{\omega^4}{\pi^2 c^3 \Delta\omega_c V_c} = Q\frac{\omega^3}{4\pi^2 c^3 V_c} \tag{6.1}$$

times more rapidly than in free space (V_c is the cavity volume) and, conversely, when the cavity is detuned from the frequency of an atomic transition the rate of radiative decay drops as the inverse of the Q-factor. After Purcell the formula for the modification of spontaneous emission by a "bad cavity" was derived many times.[62-65] It should also be noted that the quantum-mechanical amplitudes are modified by any external body (a conducting surface, nonresonant contour, etc.).[66-68] For a dipole transition we have[69]

$$w_{\mathrm{sp},ab} = \frac{4\pi}{V_c}\frac{|d_{ab}|^2}{\hbar^2}\frac{\hbar\omega_{ab}\omega_c/Q}{(\omega_{ab}-\omega_c)^2+(\omega_c^2/Q^2)},$$

$$\langle E^+E^-\rangle \equiv U(\omega) = \frac{1}{\pi V_c Q}\frac{\omega_c}{(\omega-\omega_c)^2+\Gamma_0^2}\left(\frac{\hbar\omega}{e^{\hbar\omega/kT}-1}+\frac{\hbar\omega}{2}\right), \tag{6.2}$$

where ω_c is the characteristic frequency of the cavity, ω_{ab} is the transition frequency, and d_{ab} is the transition matrix element.

When the cavity is tuned to the center of the line the probability of a radiative transition is equal to

$$w_{\mathrm{sp},ab}^{\mathrm{res}} = \frac{Q\lambda_c^3}{4\pi^2 V_c} w_{\mathrm{sp},ab}^{\mathrm{free}} \tag{6.3}$$

where $\omega_{\mathrm{sp},ab}^{\mathrm{res(free)}}$ is the probability of a transition into the cavity (into free space). When the cavity is detuned from the atomic particle by an amount ω_{ab} we obtain

$$\gamma_s = \frac{\gamma_f}{4\pi^2 Q}, \tag{6.4}$$

and γ_s can be made as small as desired. In practice it is convenient to observe precisely the slowing down of the radiative relaxation, since the acceleration of this process can be masked by collisions and transitions induced by the blackbody radiation.

We note that in the optical range, where $\lambda_c^3/V_c \ll 1$, this phenomenon is difficult, but possible, to observe.[145] Conversely, in the region of transitions between Rydberg states the phenomenon is easily observable. The first experiment of this kind was described in Ref. 41 for a beam of cesium atoms. Circular states with principal quantum number $n = 22$ and magnetic quantum number $|m| = n - 1$ were employed in the experiment. This was important, since they decay downwards in a single dipole transition $(n = 22, |m| = 21) \to (n = 21, |m| = 20)$. The wavelength was $\lambda = 0.45$ mm. In accordance with the selection rules $\Delta|m| = 1$ the radiation was polarized in a plane perpendicular to the quantization axis determined by the electric field. The beam of Rydberg atoms then passed through a capacitor formed by two flat parallel plates made of aluminum and coated with gold. The capacitor was 12.7 cm long, which gave an average passage time of the thermal atoms equal to approximately the lifetime of the Rydberg atom in free space. To reduce the effect of thermal radiation the walls were cooled to a temperature of 6.5 K. In this case the lifetime of the circular state of a cesium Rydberg atom with $n = 22$ in free space was equal to 451 μs. The distance between the plates separated by quartz disks was equal to $d = 230.1$ μm, which slightly exceeded one-half the wavelength ($d = 1.02\lambda/2$).

The idea of the experiment was as follows. Rydberg atoms in the state $n = 22$ were detected with the help of a time-of-flight detector with field ionization. The signal consisted of a time scan of the density of atoms entering the detector. The time-of-flight distribution is determined by the velocity distribution (which is Maxwellian) and the radiative decay rate, and is given by the formula[40]

$$\frac{dN}{dt} = \frac{N_0}{t_0}\left(\frac{t_0}{t}\right)^5 e^{-(t_0/t)^2}e^{-\Gamma t}, \tag{6.5}$$

where Γ is the radiative decay rate, $t_0 = L/\bar{v}$, L is the flight path, $v = (2kT/m)^{1/2}$ is the most probable velocity of atoms in the beam source, and N_0 is a normalization factor.

The parameter d was fixed, and the quadratic Stark effect was employed to vary the wavelength of the transition λ_{ab}, so that it passed through the value $\lambda_{ab}/2d = 1$. If the cavity changes the spontaneous lifetime, then in accordance with (6.5) the time-of-flight signal of the Rydberg-atom detector should also change. The typical experimental results are presented in Fig. 23. One can see that changing the parameter from the value $\lambda/2d < 1$ to $\lambda/2d > 1$ sharply changes the picture of the signal, and demonstrates the significant (by a factor of ~ 20) suppression of the rate of spontaneous decay of the circular $n = 22$ state. As a check Hulet *et al.*[40] detuned the cavity from resonance with the transition by moving the capacitor plates apart right up to $15\lambda_{ab}$. The measured lifetime of the Rydberg atoms in free space was equal to 450 ± 10 μs, which agreed very well with the computed value 451 μs at $T = 6.5$ K.

Suppression of the spontaneous emission of an atom by a cavity opens up the possibility of eliminating the natural width in spectroscopic measurements. In so doing, however, it should be remembered that a cavity unavoidably introduces energy shifts because the structure of the atom in the cavity changes, i.e., the atom-vacuum system is replaced by the atom-cavity system. It is especially important to take this effect into account when performing precise metrological measurements in the construction of frequency and time

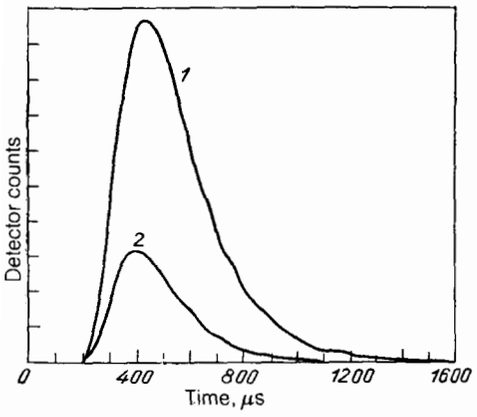

FIG. 23. The experimentally observed cavity-induced suppression of spontaneous emission.[68] The effect was recorded based on the change in the rate of radiation quenching of cesium Rydberg atoms. The time-of-flight signal at the detector of the Rydberg atoms for two cavity settings: $\lambda/2d > 1$ (1) and $\lambda/2d < 1$ (2). The signal was obtained with simultaneous modulation of the wavelength by an external electric field.

standards. Under certain conditions the processes suppressing spontaneous emission can also affect the parameters of Rydberg masers.

7. Radiation corrections. The Lamb shift in a cavity. The shift and broadening of a level by blackbody radiation. Anticrossing spectroscopy in a thermal radiation field. Modification of spontaneous emission and absorption processes results in a change in the probabilities of physical effects associated with the amplitudes of spontaneous processes. The change in the Lamb shift in a cavity is probably the most interesting effect from the physical viewpoint (but not the simplest to observe experimentally), since it can be expressed directly in terms of the sum of the amplitudes of spontaneous processes. On the other hand, the Lamb shift[69–71] (more precisely, its low-frequency part) can be regarded as a dynamic Stark effect in the vacuum polarization field. This brings the cavity-modified Lamb shift closer to another radiation correction—the dynamic Stark shift (or broadening) in a blackbody radiation field, which is more important for practical applications, for example, as an astrophysical radiometer.

Table 2 gives the hierarchy, given in Ref. 72, of physical processes which affect the Lamb shift of the $2S$ state ($\alpha = e^2/\hbar c$).

Dobiasch and Walther[72] used these estimates as the basis for studying only the change in the electron self-energy owing to the interaction with the cavity field. Such renormalization is physically related with the fact that the electron propagator in an external field[77] in free space is different from the electron propagator in the external field of a cavity mode. Unlike the radiation width (1) the resonance photons make a small contribution (which is equal to zero in the case of precise tuning to the center of the line) and the cavity operates simply as a low-frequency filter which cuts off the infrared contribution to the Lamb shift at some frequency $\omega_{cr} = 2\pi c/\lambda_{cr}$, where λ_{cr} is the critical wavelength determined by the geometry and the properties of the cavity.

This can be easily imagined, since the cavity seemingly "keeps out" of itself quantum fluctuations of the vacuum at those frequencies at which its Q-factor is adequate, with the exception of transmission bands whose statistical weight is small. Only frequencies lying in the region where the cavity no longer operates as a cavity contributes to the radiation corrections.

The effect of the renormalization of the Lamb shift is extremely small, even for cavities with a high critical frequency. For an entire series of equations it is simply equal to zero owing to the fact that the contributions of the amplitudes of the processes $nS \to (n \pm 1)P$, which have different signs, accidentally compensate one another. The corrections to the Lamb shift are greatest for those levels which lie closest to ω_{cr}, since $(n = 1)$P lies below and $(n + 1)$P above ω_{cr}. The typical magnitude of the Lamb shift is equal to

$$\delta E_{nL} = -\frac{(Ze)^2}{2n^2}\delta\omega_{cr} = 4\,(Ze)^2\frac{\mathrm{Ry}}{3n^2}\frac{r_e}{\lambda_{cr}}, \qquad (7.1)$$

where r_e is the classical electron radius. It characteristically is of the order of 10^{-4} of the total value of the Lamb shift for the level, which itself is proportional to $n^{-2.82}$ Numerically this is a very small quantity, and for the pair of transitions 23S–24P and 25S–24P it is equal to approximately 0.1 kHz. Calculation of the cavity-modified Lamb shift as a function of n gives the curve shown in Fig. 24.

It is clear from the estimates presented above that owing to the smallness of the parameter (r_e/λ_{cr}) the experimental method for observing the modification of the Lamb shift should have a resolution of tens of hertz. To realize such sensitivity a scheme for Ramsey spectroscopy in a beam of Rydberg atoms was proposed in Refs. 72 and 74. The principle of Ramsey spectroscopy consists of observing the interference of spatially separated states. The interference is ob-

TABLE II.

Order	Effect	E (2,0), MHz
$\alpha\,(z\alpha)^4$	Mass renormalization	1013.931
»	Anomalous magnetic moment	50.780
»	Vacuum polarization	—27.083
$\alpha\,(z\alpha)^5$	Relativistic corrections	7.140
$\alpha^2\,(z\alpha)^6$	Higher order corrections due to bound states	—0.354
$\alpha^2\,(z\alpha)^4$	Higher order radiation corrections	—0.072
$m_e/M_r\,(z\alpha)^4$	Corrections associated with recoil of the nucleus	—14.91
$m_e/M_r\,(z\alpha)^5$	Relativistic corrections to the recoil of the nucleus	0.342
$(R_N m)^2/(z\alpha)^4$	Finite value of the radius of the nucleus R_N	0.127
		1043.320

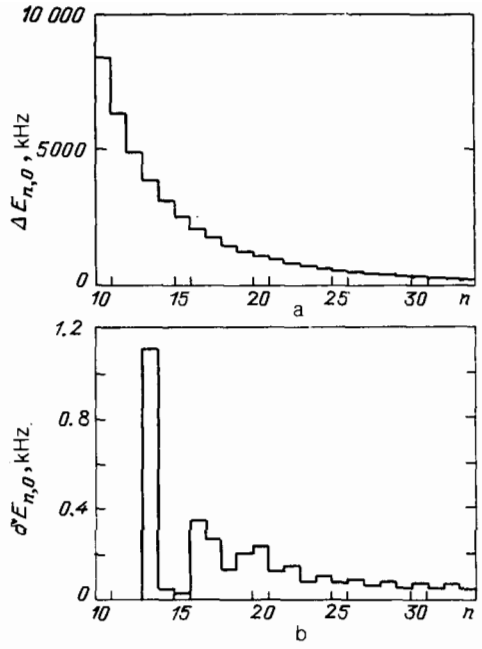

FIG. 24. The Lamb shift of the S states of the hydrogen atom for principal quantum numbers $10 \leqslant n \leqslant 40$ (Ref. 72) (a) and the absolute change in the Lamb shift in the same region but modified by the cavity, which cuts off the wavelengths at $\lambda_{cr} = 0.1$ mm (b).

served based on the beats of the population (Fig. 25). However the required measurement accuracy has not yet been achieved.

We shall now study the dynamic Stark effect from a different viewpoint, close to that presented in Refs. 75 and 76, namely, we shall determine the correction to the energy which is the sum of the spontaneous induced processes, and in addition we shall apply the fluctuation-dissipation theorem to the population of the cavity mode $U(\omega)$, which determines the contribution of induced emission. The term corresponding to the contribution of spontaneous processes contains logarithmic singularities. Unlike the contribution of spontaneous processes the contribution of induced processes diverges in a power-law fashion. However subtracting

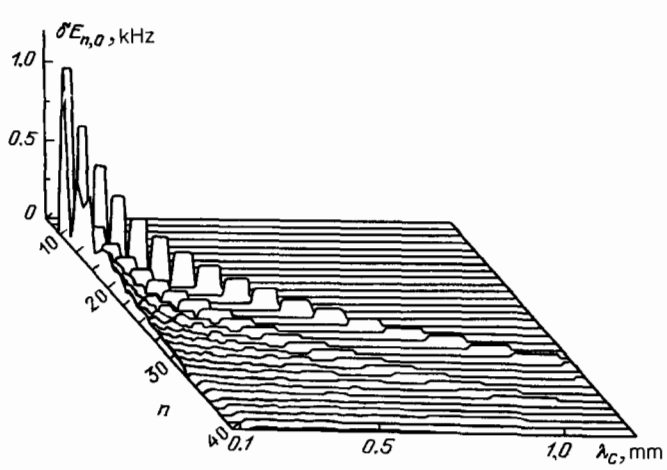

FIG. 25. The computed data on the observation of the modified Lamb shift by the method of spectroscopy of separated fields (Ramsey). The beats of the populations are recorded.

the energy of zero-point oscillations results in a finite quantity consisting of two parts: the resonance contribution of induced processes to the level shift (the effect of the order of the recoil) and the shift of the levels brought about by the blackbody radiation arising in our case as soon as we introduced the equilibrium radiation energy density ($\omega_{ab} - \omega$):

$$\delta\omega_{St}^{T} = -\frac{2}{3\pi\hbar c}\left(\sum_a \int\right)|d_{ab}|^2 \frac{(\omega_{ab}-\omega)\,d\omega}{(\omega_{ab}-\omega)^2+\Gamma_0^2} E_\omega^2$$

$$\approx \frac{e^2}{2h}\left(\sum_a \int\right)\frac{\langle r_{ab}^2\rangle \omega_{ab} E_\omega^2 d\omega}{(\omega_{ab}^2-\omega^2)}; \qquad (7.2)$$

where E_ω^2 is the intensity of the thermal-radiation field, if $\hbar\omega \lesssim kT$, which actually holds for $T = 300$ K, $n \gtrsim 15$, and at $T = 77$ K right up to $n \gtrsim 30$.

The formula (7.2) can be refined for $\hbar\omega \approx kT$; this is done in Ref. 78. We can see that Eq. (7.2) is simply the expression for the dynamic Stark shift when the frequency of the external field is much greater than the transition frequency.[79] It expresses the Joule-Lenz law with an effective "conductivity of atomic matter" $e^2/2h$. The calculations give (a more accurate analysis is performed in Ref. 76)

$$\delta\omega_{St}^{T} = \frac{e^2}{2h}\left(\sum_a \int\right)\frac{\langle r_{ab}^2\rangle\ \omega_{ab}}{\omega_{ab}^2-\omega^2} E_\omega^2 d\omega$$

$$\approx \frac{e^2}{2h}\sum_a \langle r_{ab}\rangle^2 \omega_{ab}\int \frac{E_\omega^2 d\omega}{\omega^2},$$

$$\sum_a \langle r_{ab}\rangle^2 \omega_{ab} = \frac{\hbar}{2m}. \qquad (7.3)$$

It is remarkable that this quantity is independent of both the level number and the form of the atomic potential, and is equal to 2.2 kHz. This follows mathematically from the uniqueness of the sum rules for the oscillator strengths, and physically from the fact that for $kT \gtrsim \hbar\omega$ the electron may be regarded as being free and the energy shift is equal to the shift in the field of a rapidly varying Miller force with the field intensity $\sim E_\omega^2/\omega^2$, corresponding to the intensity of the thermal-radiation field. Because the shift (7.3) is the same for all high-lying levels, in order to observe it the frequency of the transition from highly excited levels to lower-lying levels must be measured with an accuracy of the order of 10^{-12}.

When thermal radiation interacts with Rydberg atoms the levels broaden, and acquire the character of quasienergy bands.[76] The decrease in the lifetime of Rydberg states can be measured directly.[80,81] The calculation of the broadening of the levels by blackbody radiation has the form[78]

$$\Gamma_T = \frac{4}{3}\frac{k_B T}{\hbar n_a^2}\alpha^3. \qquad (7.4)$$

The lifetimes calculated from Eq. (7.4) do not depend on the angular momentum, and therefore their ratio to the spontaneous lifetimes will decrease rapidly as l increases. For interpreting the experimental results[19,81] the following facts should be kept in mind: the heat flux interacting with the atom $\sim \nu^2$ (the Rayleigh-Jeans formula) while the probability of transitions induced by the blackbody radiation is proportional to $1/n_a^2$. We find that the ratio is $\Gamma_{sp}/\Gamma_{St}^{T} \sim n^{-3}$. Figure 26 shows the measurements of the

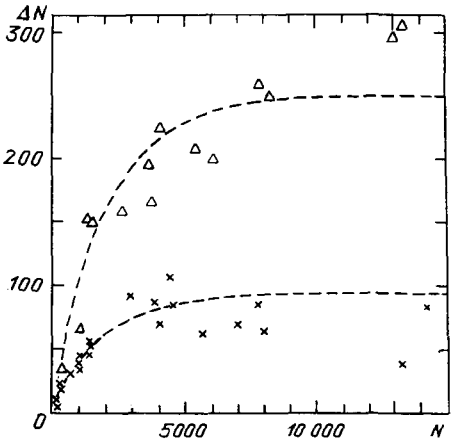

FIG. 26. The calculations and measurements (symbols) of the state populations after interaction with thermal radiation at a temperature $T = 77$ and 300 K.[81]

population of the levels after interaction with the cavity at 77 and 300 K.

The change in the lifetime of Rydberg states brought about by thermal radiation is of paramount importance for application of the Rydberg maser to the radiometry of astrophysical objects. It is well known[79] that the limit on the measurement of the brightness of radiation with a laser amplifier is

$$T_{\text{br}} \geqslant \frac{\hbar\omega_{ab}}{k \ln \xi} f, \tag{7.5}$$

where ω_{ab} is the frequency of the working transition, f is the instrumental function, and $\zeta = N_b/N_a$ is the population inversion. The possibility of operating on a maser transition with very small frequencies opens up the possibility of developing radiometers in which high sensitivity is combined with high temperature resolution. The Rydberg maser then becomes an absolute thermometer. The electron counting rate at the output is directly proportional to the temperature and does not depend on the parameters of the atom and the cavity.

The shift in the energy of an atom in a thermal radiation field is given by the formula (7.3). Therefore the shift in the per atom free energy of the atom-field system is also equal to $\delta\omega_{\text{St}}^T$, but with the opposite sign,[78] since

$$v = F - T\frac{\partial F}{\partial T}. \tag{7.6}$$

On the other hand, for low-lying levels we have $\omega_{nn'} \gg \omega_T$ and the dynamic Stark effect under the action of blackbody radiation is equal to its static value, which for a hydrogen atom is given by[16]

$$\delta\tilde{\omega}_{\text{St}}^T = \left(\sum_{n'} \frac{f_{nn'}}{4\omega_{nn'}^2}\right) \int_0^\infty F_{\omega_T}^2 d\omega_T = \frac{9}{8}\int F_{\omega_T}^2 d\omega_T, \tag{7.7}$$

$$\delta\tilde{\omega}_{\text{St}}^T = -\frac{3}{5}(\alpha\pi)^3 T^4,$$

which equals

$$\delta\tilde{\omega}_{\text{St}}^T = -\frac{3}{5}(\alpha\pi)^3 \frac{k_B T}{Ry}\frac{Ry}{\hbar}.$$

It is easy to verify that it is precisely the quantity $\delta\tilde{\omega}_{\text{St}}^T$ that, with its T^4 dependence, corresponds to the equilibrium thermal radiation in the "atom$^+$ field" system, while the expression (7.3) gives the T^2 law in complete disagreement with the thermodynamic theory of radiation. Indeed, in contradistinction to $\delta\tilde{\omega}_{\text{St}}^T$ the quantity $\delta\omega_{\text{St}}^T$ is the rms value of the shift, which is the same only in the coherence volume of a thermal quantum $\sim (kT/c\hbar)^3$ and is averaged over a large ensemble of atoms.[15] Indeed, to calculate $\delta\tilde{\omega}_{\text{St}}^T$ the statistical structure of F_ω is completely unimportant because of the inequality $\omega_{nn'} \gg \omega_T$, while the inequality $\hbar\omega \lesssim kT$ presupposes that the characteristic size of the fluctuations of the blackbody radiation field is much greater than the size of an atomic dipole $a_0 n^2 \ll k_B T/ch$; on the other hand, the temporal structure of the fluctuations is averaged over the motion of an electron along its orbit. Experiments with ensembles of atoms with characteristic linear sizes $l \lesssim kT/hc$ should thus demonstrate that owing to the partial coherence of the chaotic photon field the radiation equilibrium of such ensembles with blackbody radiation should differ from the Planck equilibrium.[67] The shifts in the energies of the levels of Rydberg atoms owing to thermal fields were observed experimentally by Hollberg and Hall.[68] The exact measurement of the shifts, which are expected to have a magnitude of ~ 2 kHz, required the application of the technology of highly stabilized dye lasers with subkilohertz linewidth. The experiments were performed by the method of Doppler-free two-photon absorption spectroscopy on the 5S–36S transition of the Rb atom using the scheme of separated optical fields[165] and the method of frequency modulation. The shift of the Doppler-free two-photon absorption resonance (top of Fig. 27) was observed in the interval of wall temperatures from 350 to 1000 K. Its width was ~ 40 kHz. The central frequency was determined with an accuracy of $\pm$ 100 Hz. Hollberg and Hall[68] clearly observed (bottom of Fig. 27) the shift which is brought about by the thermal radiation in the maximum of the resonance and which obeys the expected law $\sim T^2$. The largest magnitude of the shift at $T = 875$ K was equal to 1.42 ± 0.14 kHz. This was the first observation of the shift brought about by thermal fields in the energy of atomic states.

An interesting idea for utilizing thermal radiation in anticrossing spectroscopy of Rydberg atoms is presented in Ref. 84. Figure 28 shows a diagram of the levels of potassium for $n = 19$ and their behavior in a constant electric field. Only the top and bottom sublevels of the $n = 17$ sequence of Stark states are indicated. For $E = 550$ V/cm each Stark sublevel is a linear combination $n = 17 l \leqslant 3$ states, and the 19S state crosses the Stark sublevel with $|m_l| = 0,1$. The enlarged picture shows the appearance of pseudocrossings, and V_0 and V_1 are the energies of interaction at the crossing point.

The experiment on observation of anticrossings was arranged as follows. Potassium atoms in a thermal beam passed between two plates ($d = 1.07$cm) which formed a static electric field; in the space between the plates they were excited from the 4S ground state with the help of two (5 ns) organic-dye lasers. During a period of ~ 3 ms immediately after excitation the atoms were irradiated with thermal radiation at $T = 300$ K, which transformed $\sim 10\%$ of the excited atoms into higher states. Then they were detected with the help of the method of field ionization. The field was chosen so that the signal corresponding only to the 19P state was

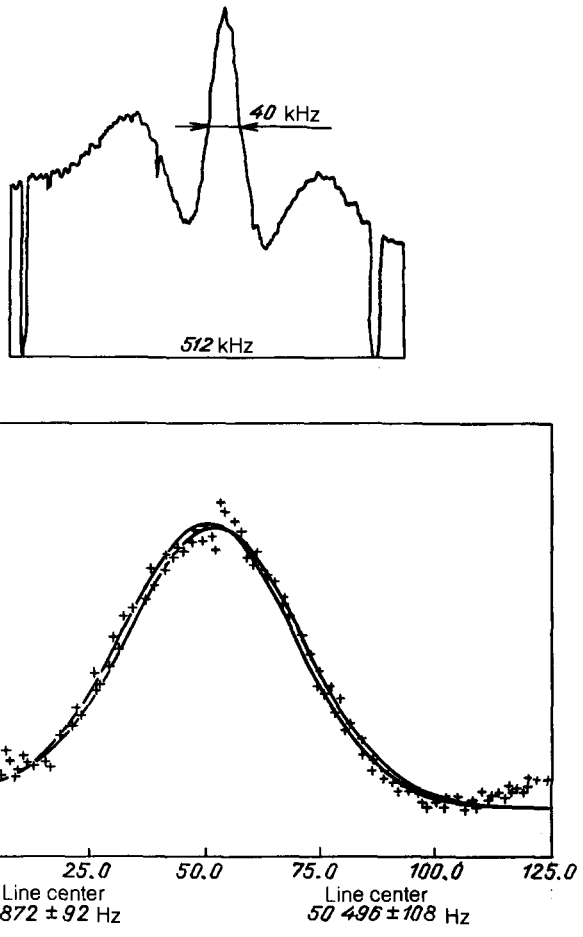

FIG. 27. The experimental measurements of the thermal-field-induced shift in the maximum of the Doppler-free resonance on the transition 5S-36S of the rubidium atom.[68] Top: two-photon absorption resonance on the transition 53–365 in rubidium; bottom: shift in the maximum of the resonance.

recorded. Assuming for the moment that the Stark states initially are not mixed, a pure Stark state cannot be excited from the 4P state by blackbody radiation. Thus one of the real states shown in Fig. 28 can be excited only through the 19P state followed by an induced transition under the action of blackbody radiation.

Let us see what happens accompanying the passage through the first pseudocrossing. Below the point of pseudocrossing the laser excites only the 19S state. There are N excited atoms. A part of γ of the atoms is transformed from the 19S state into the 19P state by the thermal radiation and gives a signal proportional to γN atoms in the 19P state. At the point of pseudocrossing the two lowest real states contain a 50% mixture (superposition) of 19S and $n = 17$ Stark states. Thus $N/2$ atoms are excited into each real state, while the total number of atoms excited by the laser remains equal to N. When the static field is changed in such a manner that a pseudocrossing occurs the number of atoms detected in the 19P state is halved and then returns to the initial value. The sharp drop in the ionic signal is shown in Fig. 29.

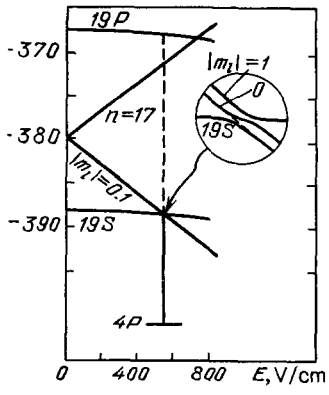

FIG. 28. Diagram of the levels of potassium, showing the crossing of the 19S state and the bottom level of the Stark shell with $n = 17$, $|m_c| = 0.1$. The broken line shows the transition into the 19P state induced by the thermal radiation.

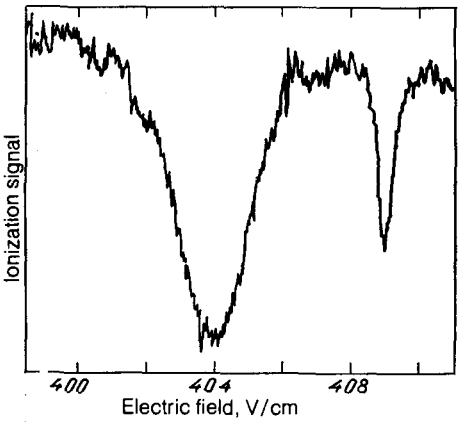

FIG. 29. Signal due to thermal-radiation-induced anticrossing of the 19S level and the ($n = 17$) Stark sublevel and recorded based on the population of the 19P state by sweeping a static electric field.

Our theoretical calculations of the non-steady-state variant of the observation of anticrossings showed that if the time of exposure to thermal radiation is much shorter than the inverse difference of the decay rates of the nS and $(n-2)$ Stark states, the anticrossing signal contains a Lorentz component and a dispersion component having the same centers and identical widths. The relative widths of the signals of these two components depend on the dipole-moment matrix elements coupling the nS and $(n-2)$ Stark states with the lower nP states.

8. Dynamics of the development of a superradiant cascade and detection of long-wavelength radiation. Collective absorption of Rydberg atoms in a cavity. The principle of detection of a microwave signal in a system of Rydberg atoms interacting with a cavity was demonstrated experimentally by Haroche's group.[59,60,83] Such detection is possible in a regime reminiscent of Dicke superradiation. In contradistinction to superradiant media in the optical range, here, because of the long wavelength of the radiation and the low thresholds, superradiation regimes are realized in media with an effective length of the order of or less than the wavelength. If the entire volume of the radiating matter falls within a half-wave of the cavity, then complete removal of the population inversion with a π pulse is possible.

Since the density of states of the electromagnetic field in the cavity is concentrated in a narrow band the nonresonant atomic transitions can be ignored and the Rydberg atom can be regarded as a two-level system. Following Refs. 5 and 59 we shall describe the theory of the superradiant regime of generation in a Rydberg maser. We introduce the characteristic times of different processes occurring in the maser. This is the characteristic decay time of the energy in an open cavity $T_c = QL/\pi C$ (for an open cavity),

$$Q = \frac{\pi R^{1/2}}{1-R} \approx \frac{\pi}{1-R},$$

and R is the reflection coefficient of the mirrors. The system is characterized by the radiation width

$$\Gamma = \frac{\omega^3 d^2}{3\pi\varepsilon_0 \hbar c^3}, \quad d \approx e a_0 n^2 \tag{8.1}$$

(the characteristic value is $\Gamma \approx 20\,\mathrm{s}^{-1}$) and the superradiant cascade time $T_R^{-1} = \Gamma N_0 \mu/2$, where $\mu \sim 1$ is the Fresnel number of the cavity, and by the splitting of the frequencies of the longitudinal modes of an open cavity $\Delta\nu_L = c/2L$.

As expected T_R is inversely proportional to the effective number of particles $(N_0\mu)$ and the decay constant of the field in the cavity $(Q\Gamma)$. The condition for the damped regime acquires the form

$$T_p \lesssim T_R, Q \lesssim \frac{\pi}{2}\left(\frac{c}{2L\Gamma N_0 \mu}\right)^{1/2}.$$

The solution in the case $\Delta z \lesssim \lambda$ has the form of the usual ch soliton:

$$\left(\frac{d\theta_0}{dt}\right)^2 = \frac{1}{4T_R^2}\,\mathrm{ch}^{-2}\,\frac{t-t_D}{2T_R}, \tag{8.2}$$

$$t_D = -2T_R \ln\frac{Q_0^i}{2}, \tag{8.3}$$

where θ_0^i is the initial value of the Bloch angle. In the theory of superradiation it is usually assumed that θ_0^i can be replaced by its rms value $\bar{\theta} = 2N^{1/2}$, reflecting the fact that in a system with the average number of particles the average fluctuation in the number of particles is equal to $\Delta N/\bar{N} = 2\bar{N}^{1/2}$. However the presence of blackbody radiation results in some differences. For $T \neq 0$ the Bloch vector "starts" from the value θ_0^i determined not only by the number of particles in the system but also by the number of blackbody radiation quanta in the mode. In some approximation θ_0^i is given by a Gaussian distribution:

$$P(\theta_0^i) = \frac{2\theta_0^i}{\bar{\theta}} \exp\left(-\frac{\theta_0^i}{\bar{\theta}^2}\right), \tag{8.4}$$

$$\bar{\theta} = \frac{2}{N_0^{1/2}(T)}, \quad N_0(T) = \frac{N_0}{1+\bar{n}_T}, \quad \bar{n}_T = (e^{\hbar\omega/k_B T} - 1)^{-1},$$

which corresponds to the applicability of the central limit theorem to fluctuations of the dipole moment. The probability distribution for the quantity t_D has the form

$$P(t_D) = \frac{N_0(T)\exp(-t_D/T_R)}{T_R} \exp(-N_0(T)\,e^{-t_D/T_R}). \tag{8.5}$$

For the average value of variance of the delay time we have

$$\langle t_D\rangle = T_R \ln N_0(T) = T_R \ln\frac{N_0}{1+n_T}, \tag{8.6}$$

$$\Delta t_D = (\langle t_D^2\rangle - \langle t_D\rangle^2)^{1/2} \approx 1.3 T_R. \tag{8.7}$$

The appearance of the temperature dependence of t_D is actually connected with the following fact. Several quanta of thermal radiation are sufficient to start a superradiant cascade. At the same time the phenomenon of photon bunching is characteristic for thermal radiation, i.e., the probability of the appearance of photons immediately after a given photon increases, while the variance of the distribution is larger than for a Poisson distribution. To determine the generation threshold of a Rydberg maser the following must be taken into account: 1) decay of the working level into other states, both spontaneous decay and decay induced by blackbody radiation; 2) collisional depopulation of the working level; 3) the parasitic effects of external fields; and, 4) effects associated with the motion of atoms in the beam. Under the conditions of the experiments of Refs. 59 and 60, because of the low working densities of the selectively excited Rydberg atoms and the high vacuum collisional deexcitation did not play a significant role. The characteristic thermal radiation of the cavity can be effectively suppressed by working at low temperatures. In this case the threshold is determined by transport of active atoms away from the caustic of the cavity mode. This results in the inequality

$$T_R \ln\frac{N_0}{1+\bar{n}_T} \lesssim T_t^* = \frac{\sqrt{2}\omega_0}{\bar{v}} \approx 10^{-5}\,\mathrm{s}. \tag{8.8}$$

For $\bar{v} = 890$ m/s, $\omega_0 \approx 1$ cm $\bar{n}_T \ll N_0$. This inequality actually determines the number of atoms which can be found in the inverted state. For $Q \sim 100$ the inequality (8.8) gives several hundred atoms for the number N_0.

Let us consider the effect of external injected radiation on the characteristics of a Rydberg maser. We introduce the parameter $\eta = (\theta_1/\bar{\theta})^2$:

$$\eta = \frac{(\Omega_c^{tr})^2}{1+(2\Delta\omega T_R)^2} N_0 T_R^2 = \frac{1}{1+(2\Delta\omega T_R)^2}\frac{T_R}{T_c} n_c^{tr}, \tag{8.9}$$

$$n_c^{tr} = \frac{\pi\varepsilon_0\varepsilon_{tr}^2}{8}\frac{L\omega_0^2}{\hbar\omega}, \quad \Omega_c^{tr} = \frac{|d\varepsilon_{tr}|}{\hbar} \ll T_R^{-1}.$$

This parameter determines the ratio of the number of photons of the injected field ε_{tr} to the quantity

$$\left(\frac{T_R}{T_p}\right)^{-1} = \frac{2Q}{\pi}\frac{\Gamma}{\Delta v_i}N_0\eta,$$

characterizing the external numbers of superradiated photons in the cavity band above the minimum noise of the amplifier "one photon per mode," taking into account the detuning from resonance. Thus the parameter η^2 determines the ratio of the effectiveness of the injected signal to the effectiveness of the amplifier noise as a seed for superradiation.

For the starting level determined by the equality (8.7) at $t = 0$ we shall redefine the "Bloch vector" as follows:

$$\theta^e e^{i\phi_e}|_{t=t_0} = e^{t\phi_i}\theta_0^! + \theta_1, \tag{8.10}$$

and we shall use this value of the new "Bloch vector" as the initial condition in the theory of superradiation:

$$\theta^e e^{i\phi_e}|_{t=t_0} = e^{t_0/2T_R}\theta e e^{i\phi_e}|_{t=0}, \tag{8.11}$$
$$t_0 < T_R \ln N_0.$$

From here we have

$$t_D = -2T_R \ln\frac{\theta_e}{2}, \quad \langle\theta^e\rangle = \bar{\theta}(1+\eta^2)^{1/2},$$
$$\langle t_D(\eta)\rangle = T_R \ln\frac{N_0}{1+\eta^2}, \tag{8.12}$$
$$\Delta t_D(\eta) = (\langle t_D^2\rangle - \langle t_D\rangle^2)^{1/2} \approx 2\bar{\theta}T_R\frac{\partial}{\partial\theta^e}\ln\frac{\theta^e}{2} = \frac{2R}{(1+\eta^2)^{1/2}}$$

[the more accurate numerical coefficient is $1{,}3T/(1+\eta^2)^{1/2}$].

Because of the low spontaneous times a Rydberg maser is triggered by photons of thermal radiation, whose fluctuations determine the dynamics of the development of generation. It is obvious that a Rydberg maser can also be triggered by an external applied resonant microwave field. In this case such a system will be a microwave radiation detector. The following scheme is realized for obtaining maximum sensitivity (Fig. 30).[58]

The atoms in the tuned resonator are two-level systems

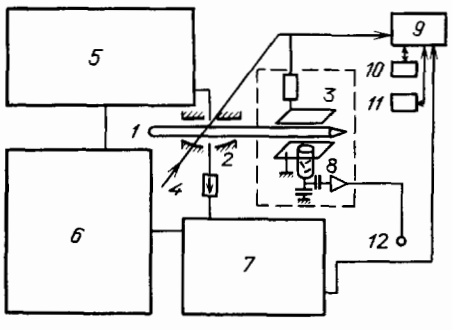

FIG. 30. The experimental arrangement of a trigger-initiated Rydberg maser.[5] 1—Atomic beam, 2—microwave resonator, 3—Rydberg atom detector based on field ionization, 4—laser radiation, 5—klystron generator, 6—stabilization and frequency multiplication unit of klystron generator, 7—heterodyne receiver, 8—electron multiplier, 9—fast digital oscillograph, 10—automatic plotter, 11—boxcar, 12—ionization-current meter.

in two independent states. Some atoms are prepared in the $|nS_{1/2}, m_J = -1/2\rangle$ state and undergo a transition to the $|n'P_{1/2}, m_J = 1/2\rangle$ sublevel. Other atoms are excited into the $|nS_{1/2}, m_J = +1/2\rangle$ state and undergo a radiative transition to the $|n'P_{1/2}, m_J = -1/2\rangle$ sublevel. These two independent groups of atoms emit orthogonal σ^+ and σ^- circularly polarized waves. In a "spontaneous" maser, i.e., a maser triggered by spontaneous radiation, both components are emitted independently with uncorrelated phases. The resulting field is elliptically polarized—almost linearly polarized throughout virtually the entire time of development of generation. The major axis of the ellipse rotates randomly by small angles around the axis of the cavity from one pulse to another. The average power detected through a rectangular waveguide is equal to one-half the emitted power.

On the other hand, if linearly polarized radiation interacts with the atoms, the two oppositely rotating components of the polarization are synchronized in phase and the maser generates linearly polarized radiation in the same plane. Figure 31 shows a block diagram of the triggering of a maser with different polarizations.[58] The circular input waveguide transmits any linear polarization. If it is parallel to the small dimension of the rectangular waveguide, 100% of the generation pulses can be detected.

In the case when the maser is triggered by external microwave radiation the delay time of generation is shortened and phase and polarization locking are observed. The number of photons required for triggering the maser is determined by the quantity

$$n_c^{tr} = \frac{T_R}{T_c}n_c \tag{8.13}$$

where $T_c = Q/2\pi\nu_c$ and n_c is the number of microwave photons accumulated in the cavity and is related with the incident microwave power and the Q-factor of the cavity by the relation

$$n_c = \frac{P_n Q}{2\pi h\nu^2}. \tag{8.14}$$

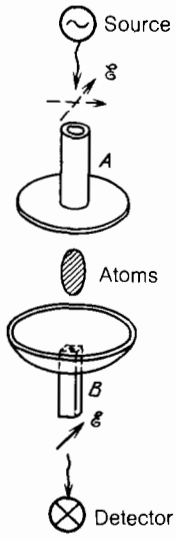

FIG. 31. Block diagram of polarization detection of microwave radiation in a trigger-initiated maser.

The limit of sensitivity of such a trigger maser detector is determined from the condition that the number of photons necessary for triggering the maser n_c^{tr} over the time period of development of generation T_R is of the order of or somewhat less than the number of thermal-radiation photons in the interval $\Delta\nu$, i.e., $k_B T/h\nu$. For a cavity with $T_R/T_c = 10$ shortening of the delay with on the average not more than one photon in the cavity $n_c = 1$, $n_c^{tr} = 10$, was observed experimentally in Ref. 59. This corresponded to output power $P = 10^{-14}$ W and a detection sensitivity $3\cdot 10^{-18}$ W/Hz$^{1/2}$ in a band having a width 10^7 Hz $= T_c^{-1}$. In addition this sensitivity was achieved with the surrounding walls at room temperature. Cooling to the temperature of liquid nitrogen ($T = 77$ K) or the temperature of liquid helium (4 K) should undoubtedly greatly increase the sensitivity.

In Ref. 60 the trigger scheme was realized with a small number of Na atoms ($1 < N < 10^5$). The operation of the Rydberg maser was ensured by increasing the Q-factor of the microwave cavity. Decreasing the density of atoms resulted in the fact that, being located in the antinode of a standing wave, they behave like a superradiant system, i.e., they exhibit collective effects. Among such effects we mention the saturation of the ratio $\Delta N/N$, where ΔN is the number of atoms which have absorbed photons from the signal and N is the total number of atoms; this property is important for a detector. As a result it turned out that N has both a lower limit and an upper limit, i.e., there is an optimal value. In this work the best results for detection were as follows: $P = 10^{-15}$ W and NEP $= 10^{-18}$ W/Hz (at 134 and 270 GHz at $T = 6$ K).

The collective absorption by a system of Rydberg atoms was employed in Ref. 59 to demonstrate the possibilities of using a Rydberg maser as an absolute thermometer. It was found that in the case of a $30S_{1/2}$–$30P_{1/2}$ transition in Na atoms ($\nu = 134$ GHz, $\lambda = 2.25$ mm, and $h\nu/k_B = 6.45$ K) induced by thermal radiation the atomic system absorbs a fixed number of blackbody photons in the cavity, and the number of induced transitions ΔN, on the one hand, can be much greater than the quantity $\Delta N_1 = W_T^p \tau_{int}$, where $W_T^p = (\pi d^2/\hbar^2) I_T^p$, I_T^p is the energy density of states in a mode at exact resonance $I_T^p = (\hbar Q/\pi\nu)\bar{n}$, and τ_{int} is the time of interaction with the cavity, while on the other hand it is much less than the quantity

$$\Delta N_2 = \bar{n}_T \frac{Q}{2\pi\nu} \tau_{int}, \quad \Delta N_1 \ll \Delta N \ll \Delta N_2,$$

so that only a small fraction of the photons emitted by the cavity over the time of interaction is absorbed by the atomic system. The mechanism of absorption by the system of Rydberg atoms thus exhibits a collective character, namely, under the action of the resonance blackbody radiation field the atomic dipoles are brought in phase, and the system of atoms concentrated in a small (compared with wavelength) spatial region behaves as a quantum object with nondegenerate energy states and a dipole moment which is proportional to the total number of atoms. The characteristic time of the collective process is $T_R^{-1} \approx (d^2/\hbar V) QN$ and the number of induced transitions is $\Delta N_1 = (T_R/\tau_{int}) = W_T^p T_R N = n_T$ and is independent of both the properties of the resonator and the parameters of the system. This property of collective induced absorption by ensembles of Rydberg atoms also permits constructing an absolute thermometer directly by measuring the number of particles which have undergone a transition induced by blackbody radiation.

The fact that Δn is independent of the properties of the atoms and the cavity if $V_{at} \ll \lambda^3$ suggests that it is possible to derive an expression for Δn based on general statistical arguments. Indeed, an atomic system has $N + 1$ symmetric excited states corresponding to a quantum on one of the excited atoms.

Thus a system of N atoms in a cavity with an oscillator mode is equivalent to a supersymmetric harmonic oscillator[132,133] if it is initially prepared in a symmetric state. For this reason, in the state of thermodynamic equilibrium it is characterized by a single quantity—the occupation number with the equilibrium temperature T. However each state is additionally doubly degenerate with respect to the state of photon polarization: the transition $30S_{1/2} - 30P_{1/2}$ has two components:

$$|30S_{1/2}, m_J = \pm\frac{1}{2}\rangle \xrightarrow{\sigma_+\ \sigma_-} |30P_{1/2}, \quad m_J = \mp\frac{1}{2}\rangle \text{ and } \Delta n = 2\bar{n}_T.$$

In this intuitive picture it is not too clear how the phased atomic dipoles evolve under the action of a black body. To elucidate this we shall employ the model of a global Bloch vector of a system of $N/2$ atoms, which initially is in the "down" state (the ground state of the atomic system). The moving Bloch vector is described by three averages of the angular momentum operators: $J_{x,y,z}$. Under the action of blackbody radiation the quantities $J_{x,y}$ acquire the value $J_i = N\theta_i/4 (i = x,y)$ where θ_i are small values of the fluctuating Bloch angle.

Since the total angular momentum is conserved J_z changes by the amount $\Delta J_z = N(\theta_x^2 + Q_y^2)/8$. The motion of the Bloch vector is identical to the motion of a Brownian particle with velocity $v_i = c\theta_i$ and mass $m = N\hbar\nu/2c^2$ with damping $\sim T_R/2$ and the fluctuating force $F(t)/mc = dE_T^i(t)/\hbar$ with a correlation time $T_c \ll T_R$. For this reason in a "bad" cavity the action of blackbody radiation can be interpreted as δ-correlated points, as a result of which the particle (the tip of the representative Bloch vector) acquires the kinetic energy

$$\varepsilon_{kin} = \frac{mv^2}{2} = \frac{N\hbar\nu^2}{4}\theta_i^2 = \frac{k_B T}{2}.$$

We have

$$2(\Delta J_z)_c = \frac{N}{4}(\theta_x^2 + \theta_y^2) = \frac{k_B T}{h\nu}.$$

If $\tau_{int} < T_R$, then Δn is given by the formula $\Delta n = 2\bar{n}_T(1 - e^{-\tau_{int}/T_R})$, so that the time over which thermodynamic equilibrium is achieved between the field and the atoms is inversely proportional to N. The fluctuations var $(\Delta n) = (\langle\Delta n^2\rangle - \langle\Delta n\rangle^2)^{1/2}$ from one beam of collective absorption to another are determined by the Bose-Einstein statistics, though each atom is described by a fermion degree of freedom, and are equal to var $(\Delta n) = 2\bar{n}(1 + 2\bar{n}_T) \approx 4n_T^2 (\bar{n}_T \gg 1)$. These phenomena are of a completely general character. But only the very large values of $\tau_{int}/T_R \sim d^2$ characteristic for systems of Rydberg atoms

and the small values of N as well as the possibility of placing a system of N atoms in a volume $V_{aT} \ll \lambda_0^3$, i.e., in practice either at the node or at an antinode of the cavity, make it possible to observe these effects with finite detection accuracy $\Delta n/N$. An exact theory of collective absorption by atoms in a cavity, based on the density matrix formalism, is given in Ref. 61.

The effect of superradiation is well known for another type of system with a small number of electrons—weakly relativistic Landau electrons interacting through a cavity mode. The anharmonicity of the quantum oscillators results in phasing of their initially unphased oscillations and in the formation of a state with a dipole moment proportional to the total number of radiating systems. The initially excited oscillators, interacting through the characteristic radiation field, are in an unstable state. A small fluctuation of the average polarization, just as in the case of a two-level system, initiates the development of this instability and results in exponential growth of the radiation intensity. In a system of linear oscillators the average polarization decays exponentially. The nonlinearity limits this growth and forms a superradiant pulse.[135]

IV. CONCLUSION

It is obvious from this review that the last few years were a period of intense experimental and theoretical study of the radiation of properties of Rydberg atoms. The experimental realization of quantum-electronic devices such as the one-atom maser and the two-photon micromaser, and the observation of the subtle effects of thermal radiation have confirmed the uniqueness and very extensive possibilities of Rydberg atoms as an object of quantum optics. It is now possible to study experimentally the effects predicted long ago before Rydberg masers were developed and which at that time appeared to be of purely theoretical significance. This includes the change in the rate of spontaneous emission of one atom placed in a cavity, the oscillator character of the exchange of energy between one excited atom and a cavity mode, and quantum decay and revival of optical notations induced in one atom by the resonance field. Successful experiments are possible for the following basic reasons. First, the coupling of the atoms with the electromagnetic field is strong owing to the gigantic dipole moments of the transitions. Second, millimeter-range radiation is employed; this has made it possible to build cavities which have low-order modes and at the same time are large enough to provide long interaction times. Third, the long spontaneous lifetimes of atoms in Rydberg states became important; this has made it possible to perform precise spectroscopic measurements. And, finally, atomic beams and tunable lasers are used for efficient excitation of Rydberg atoms with selection by states and field ionization is employed to detect them sensitively.

It is also clear that new experimental discoveries, made possible by the specific nature of the range of electromagnetic radiation employed, the possibility of manifestation of coherent and collective effects, and the unusual correlation and statistical properties, can be expected in the near future. It is possible that experiments will be able to make use of the unusual properties of the Rydberg atom on the surface of liquid helium.

The results of these investigations will not be merely of academic interest. There is no doubt that many of them will find application in metrology, for solving the problem of sensitive detection of microwave radiation, measuring superweak electric fields and their fluctuations, and studying surfaces. Other unexpected applications are also possible. For this reason we believe that the investigations described here are just beginning and are merely opening up a new and intriguing field of quantum optics.

Finally, we would like to thank H. Walther and N. B. Delone for stimulating our interest in this subject, and N. B. Delone, V. P. Kraĭnov, and V. M. Smirnov for numerous valuable remarks and suggestions.

One of us (P. L.) thanks K. K. Likharev for the idea of writing this review and P. V. Elyutin and M. S. Maslova for explaining a number of theoretical questions.

[1] New methods for obtaining Rydberg states with a large projection of the angular momentum in crossed electric and magnetic fields and with stochastic collisions were recently proposed in Ref. 160 and 161, respectively.

[1] D. Meschede, H. Walther, and G. Muller, Phys. Rev. Lett. **54**, 551 (1985).
[2] G. Rempe *et al.*, *Proceedings of the 6th International School on Coherent Optics*, September 19–26, 1985, Poland (1985).
[3] P. Filipovicz *et al.*, Opt. Acta **32**, 1105 (1985).
[4] P. Goy *et al.*, Phys. Rev. Lett. **50**, 1903 (1983).
[5] L. Moi *et al.*, Phys. Rev. A **27**, 2043 (1983).
[6] M. L. Zimmerman *et al.*, *ibid.* A **27**, 2731.
[7] L. M. Humprey *et al.*, *ibid.* **20**, 2251 (1979).
[8] T. F. Gallagher *et al.*, *ibid.* **23**, 2065 (1981).
[9] M. Brune *et al.*, Phys. Rev. Lett. **59**, 1899 (1987).
[10] E. M. Purcell, Phys. Rev. **69**, 681 (1946).
[11] F. W. Cummings, *ibid.* A **140**, 1051 (1965).
[12] R. H. Dicke, Phys. Rev. **93**, 99 (1954).
[13] M. B. Bell and E. R. Seaquist, Astrophys. J. **238**, 818 (1980).
[14] V. Mebold *et al.*, Astrophys. J. Lett. **82**, 272 (1980).
[15] A. A. Ershov *et al.*, Pis'ma Astron Zh. **10**, 833 (1984) [Sov. Astron. Lett. **10**, 348 (1984)].
[16] R. F. Stebbings and F. B. Dunning [Eds.], *Rydberg States of Atoms and Molecules*, Cambridge Univ. Press, 1983, [Russ. transl., Mir, M., 1985.]
[17] B. M. Smirnov, *Excited Atoms* [in Russian], Énergoatomizdat, M., 1982.
[18] N. B. Delone, V. P. Kraĭnov, and D. L. Shepelyanskiĭ, Usp. Fiz. Nauk **140**, 355 (1983) [Sov. Phys. Usp. **26**, 551 (1983)].
[19] J. Gallas *et al.*, Adv. Atom. Mol. Phys. **20**, 413 (1985).
[20] R. A. Sorochenko and G. G. Smirnov, Pis'ma Astron Zh. **13**, 191 (1987) [Sov. Astron. Lett. **13**, 77 (1987)].
[21] C. Leonard and R. H. Rinkleff, Phys. Lett. A **112**, 208 (1985).
[22] A. N. Klyucharev and N. N. Bezuglov, *Excitation and Ionization of Atoms Accompanying the Absorption of Light* [in Russian], Leningrad State University Press, Leningrad (1983).
[23] C. E. Theodosiou, Phys. Rev. A **30**, 2881 (1984).
[24] I. M. Beterov *et al.*, Zh. Eksp. Teor. Fiz. **93**, 31 (1987) [Sov. Phys. JETP **66**, 17 (1987)].
[25] I. M. Beterov *et al.*, Z. Phys. D **6**, 55 (1987).
[26] T. W. Ducas *et al.*, Phys. Rev. Lett. **35**, 366 (1975).
[27] R. V. Ambartsumyan *et al.*, Pis'ma Zh. Eksp. Teor. Fiz. **21**, 595 (1975) [JETP Lett. **21**, 279 (1975)]; Zh. Eksp. Teor. Fiz. **73**, 157 (1977) [Sov. Phys. JETP **46**, 81 (1977)].
[28] C. Fabre *et al.*, Phys. Rev. A **18**, 229 (1978).
[29] P. M. Koch, Phys. Rev. Lett. **43**, 432 (1979).
[30] C. Fabre *et al.*, Opt. Commun. **13**, 393 (1975).
[31] D. Tuan *et al.*, *ibid.* **18**, 533 (1976).
[32] B. G. Zollars *et al.*, J. Chem. Phys. **84**, 5589 (1986).
[33] S. A. Lee *et al.*, Opt. Lett. **3**, 141 (1976).
[34] L. S. Vasilenko, V. P. Chebotaev, and A. V. Shishaev, Pis'ma Zh. Eksp. Teor. Fiz. **12**, 161 (1970) [JETP Lett. **12**, 113 (1970)].
[35] V. S. Letokhov and V. P. Chebotaev, *Nonlinear Laser Spectroscopy*, [Russ. original, Nauka, M., 1975].
[36] R. Beigang and A. Timmerman, Phys. Rev. A **26**, 2990 (1982).
[37] R. Beigang *et al.*, Opt. Commun. **49**, 253 (1984).
[38] J. H. M. Nielsen *et al.*, Physica B + C **111**, 127 (1981).
[39] I. M. Beterov, V. L. Kurochkin, and I. G. Yudelevich, Zh. Prikl. Spek-

trosk. **42**, 17 (1985). [J. Appl. Spectrosc. **42**, 11 (1985)].
[40] R. C. Hulet *et al.*, Phys. Rev. Lett. **55**, 2137 (1985).
[41] R. C. Hulet and D. Kleppner, *ibid.* **51**, 1480 (1983).
[42] J. Liang *et al.*, Phys. Rev. A **33**, 4437 (1985).
[43] M. Gross, J. Liang *et al.*, Phys. Rev. Lett. **57**, 1160 (1986).
[44] A. I. Baz', Ya. B. Zel'dovich, and A. M. Perelomov, *Scattering, Reactions, and Decay in Nonrelativistic Quantum Mechanics*, Wiley, N.Y. 1969. [Russ. original Nauka, M., 1971 2nd ed. p. 39].
[45] N. B. Delone *et al.*, Izv. Akad. Nauk SSSR, Ser. Fiz. **48**, 682 (1984). [Bull. Acad. Sci. USSR. Phys. Ser. **48**, (1), 56 (1984)].
[46] J. E. Bayfield and L. A. Pinnaduwage, Phys. Rev. Lett. **54**, 313 (1985).
[47] R. Blumel *et al.*, Z. Phys. D **6**, 83 (1987); **9**, 95 (1988).
[48] P. M. Koch *et al.*, *Physics of Phase Space*, Springer-Verlag, N.Y. 1987, p. 37 (Lecture Notes in Physics, Vol. 3).
[49] R. V. Jensen, Phys. Rev. A **30**, 386 (1984).
[50] J. G. Leopold and D. Richards, J. Phys. B **18**, 3369 (1985); **19**, 1125 (1986).
[51] G. Casati *et al.*, Phys. Rev. Lett. **57**, 823 (1986).
[52] G. Casati *et al.*, **59**, 2729 (1987).
[53] D. L. Shepelyansky, Preprints, Institute of Nuclear Physics 86–29, 86–187, 87–30, Novosibirsk (1986, 1987).
[54] G. Casati *et al.*, Preprints, Institute of Nuclear Physics 87–29, 87–30, Novosibirsk (1987).
[55] J. N. Bardsley and B. Sundaram, Phys. Rev. A **32**, 689 (1985).
[56] R. Blumel and U. Smilansky, *ibid.*, 1900.
[57] I. Ya. Bersons, Zh. Eksp. Teor. Fiz. **83**, 1276 (1982) [Sov. Phys. JETP **56**, 731 (1982)]. Preprint LAFI–109, Institute of Physics, Academy of Sciences of the Latvian SSR, Salaspils (1987).
[58] P. Goy, *Infrared and Millimeter Waves*, edited by K. J. Button, Academic Press, N.Y., Vol. 8, Part 1, p. 342.
[59] P. Goy *et al.*, Phys. Rev. A **27**, 2065 (1983).
[60] P. Goy *et al.*, J. Appl. Phys. **56**, 627 (1984).
[61] K. H. Drexhage, Prog. Opt. **12**, 165 (1985).
[62] N. Bloembergen and R. W. Pound, Phys. Rev. **95**, 8 (1954).
[63] M. W. Stranberg, *ibid.* **106**, 617 (1957).
[64] F. V. Bunkin and A. N. Oraevskiĭ, Izv. Vyssh. Uchebn. Zaved., Radiofiz. **11**, 81 (1959).
[65] P. B. Lerner, Preprint No. 315, Physics Institute of the Academy of Sciences of the USSR, Moscow (1986).
[66] V. P. Bykov and G. V. Shepelev, *Radiation of Atoms and Molecules Near Material Bodies: Problems in Quantum Theory* [in Russian], Nauka, M., 1986.
[67] S. M. Rytov, *Introduction to Statistical Radio Physics* [*in Russian*], Nauka, M., 1966.
[68] M. Hollberg and J. L. Hall, Phys. Rev. Lett. **53**, 230 (1984).
[69] W. Heitler, *The Quantum Theory of Radiation* 3rd Ed., Clarendon Press, Oxford, 1954. [Russ. transl., Inostr. Lit., M., 1956].
[70] V. M. Fain, Izv. Vyssh. Uchebn. Zaved., Radiofiz. **11**, 167 (1959).
[71] S. Sachdev, Phys. Rev. A **29**, 2627 (1984).
[72] P. Dobiasch and H. Walther, Ann. Phys. **10**, 825 (1985).
[73] S. S. Schweber, *An Introduction to Relativistic Quantum Field Theory*, Row, Peterson and Company, Evanston, IL. 1961 [Russ. transl., Inostr. Lit., M., 1963].
[74] J. Krause, M. Scully, and H. Walther, Phys. Rev. A **34**, 2032 (1986).
[75] T. Welton, *ibid.* **74**, 1157 (1948).
[76] G. W. Ford *et al.*, *ibid.* **34**, 2001 (1986).
[77] V. B. Berestetskiĭ, E. M. Lifshitz, and L. P. Pitaevskii, *Quantum Electrodynamics*, Pergamon Press, Oxford, 1982; [Russ. original Nauka, M., 1980].
[78] J. W. Farley and W. H. Wing, Phys. Rev. A **23**, 2397 (1981).
[79] C. H. Townes and A. L. Shawlow, *Microwave Spectroscopy*, McGraw–Hill, N.Y., 1955. [Russ. trans., Inostr. Lit., M., 1959].
[80] P. M. Koch *et al.*, Phys. Lett. A **75**, 273 (1980).
[81] T. F. Gallagher and W. E. Cooke, Phys. Rev. Lett. **42**, 835 (1979).
[82] H. A. Bethe and E. E. Salpeter, *Quantum Mechanics of One- and Two-Electron Systems*, Springer Verlag, Berlin, 1958. [Russ. transl. Fizmatgiz, M., 1960].
[83] S. Haroche and J. M. Raimond, Adv. Atom. Mol. Phys. **20**, 347 (1985).
[84] R. C. Stoneman *et al.*, Phys. Rev. A **34**, 2952 (1986).
[85] E. T. Jaynes and F. W. Cummings, Proc. IEEE **51**, 89 (1963).
[86] P. B. Lerner and I. M. Sokolov, Pis'ma Zh. Eksp. Teor. Fiz. **44**, 501 (1986) [JETP Lett. **44**, 644 (1986)].
[87] J. H. Eberly *et al.*, Phys. Rev. Lett. **40**, 1323 (1980).
[88] J. Eberli, N. B. Narozhnyĭ, and R. Sanches-Mondragon, Kvant. Elektron. 7, 2178 (1980) [Sov. J. Quantum Electron. **10**, 1261 (1980)].
[89] H. I. Yoo and J. H. Eberly, Phys. Rep. **118**, 239 (1985).
[90] S. M. Burnett and P. L. Knight, Phys. Rev. A **33**, 2444 (1986).
[91] G. S. Agarwall and S. Puri, *ibid.*, 1757, 3610.
[92] G. S. Agarwall and S. Puri, *ibid.* **35**, 8 (1987).
[93] H. Walther, Atom. Phys. **10**, 333 (1987).
[94] G. Rempe, H. Walther, and N. Klein, Phys. Rev. Lett. **58**, 353 (1987).
[95] P. Filipowich *et al.*, J. Opt. Soc. Am. **13**, 906 (1986).
[96] J. Acherhalt, Phys. Rev. Lett. **50**, 966 (1983).
[97] B. V. Chiricov, Phys. Rep. **52**, 263 (1979).
[98] R. F. Fox and J. Edison, Phys. Rev. A **34**, 482 (1986).
[99] D. L. Shepelyansky, Phys. Rev. Lett. **57**, 15 (1986).
[100] P. Meystre *et al.*, Nuovo Cimento B **25**, 12 (1975).
[101] P. Meystre and M. S. Zubairy, Phys. Lett. A **89**, 390 (1982).
[102] H. J. Carmichael, Phys. Rev. Lett. **55**, 2790 (1985).
[103] M. Hillery *et al.*, Phys. Lett. A **103**, 259 (1986).
[104] H. Paul, Rev. Mod. Phys. **54**, 1061 (1982).
[105] H. J. Carmichael, Phys. Rev. A **33**, 3262 (1986).
[106] A. S. Shumovskiĭ and V. I. Yukalov, *Proceedings of the International School on High Energy Physics*, Joint Institute of Nuclear Research, Dubna (1983).
[107] F. W. Cummings and A. Dorri, Phys. Rev. A **28**, 2282 (1983).
[108] F. W. Cummings, *ibid.* **33**, 1683 (1986).
[109] C. R. Stroud *et al.*, *ibid.*, **5**, 1094 (1972).
[110] P. Kulina, C. Leonard, and R. H. Rinkleff, *ibid* **34**, 227 (1986).
[111] G. P. Hildred *et al.*, J. Phys. B. **17**, L535 (1984).
[112] P. Filipowich *et al.*, Phys. Rev. A **34**, 3077 (1986).
[113] J. Liang, M. Gross, and S. Haroche *ibid* **33**, 4437.
[114] P. L. Knight and P. M. P. M. Radmore, Phys. Lett. A **90**, 342 (1982).
[115] M. Brune, J. M. Raimond, and S. Haroche, Phys. Rev. A **35**, 154 (1987).
[116] P. L. Knight, Phys. Scripta **12**, 51 (1986).
[117] L. Davidovich *et al.*, Phys. Rev. A **36**, 3771 (1987).
[118] L. A. Lugiato *et al.*, *ibid.*, 740.
[119] M. S. Abdalla *et al.*, *ibid.* **34**, 4829 (1986).
[120] A. M. Prokhorov, Science **149**, 828 (1965).
[121] V. S. Letokhov, Pis'ma Zh. Eksp. Teor. Fiz. 7, 284 (1968) [JETP Lett. **7**, 221 (1968)].
[122] M. P. Yuen, Phys. Lett. A **51**, 1 (1975).
[123] C. Cohen-Tannoudji and S. Reynaud, J. Phys. B **10**, 345 (1977).
[124] P. L. Knight and P. W. Milloni, Phys. Rep. **66**, 21 (1980).
[125] P. A. Apanasevich, *Foundations of Theory of Interaction of Light with Matter* [in Russian], Nauka i tekhnika, Minsk (1977).
[126] L. E. Gendenshteĭn and I. E. Krive, Usp. Fiz. Nauk **146**, 554 (1985).
[127] Y. Aharonov *et al.*, Phys. Rev. D **29**, 2396 (1984).
[128] P. van Nieuwenhuizen, Phys. Rep. **68**, 189 (1981).
[129] G. S. Agarwall, *Springer Tracts in Modern Physics* (1986), p. 53.
[130] S. Haroche, *New Trends in Atomic Physics*, edited by R. Hora and G. Grynberg, North-Holland, Amsterdam (1984).
[131] E. Witten, Nucl. Phys. B **185**, 513 (1981).
[132] R. Loudon, *The Quantum Theory of Light*, Clarendon Press, Oxford, 1973 [Russ. transl., Mir, M., 1976].
[133] P. Lerner and N. Maslova, Preprint No. 77, Physics Institute of the Academy of Sciences of the USSR, Moscow (1987).
[134] D. A. Leites, Usp. Mat. Nauk **35**, 24 (1980). [Russ. Math. Surv. **35**, 1 (1980)].
[135] Yu. A. Il'inskiĭ and N. S. Maslova, Zh. Eksp. Teor. Fiz. **94**, 171 (1988) [Sov. Phys. JETP **67**, 96 (1988)].
[136] M. Lax, Phys. Rev. **172**, 1490 (1968).
[137] D. F. Smirnov and A. S. Troshin, Usp. Fiz. Nauk **153**, 233 (1987) [Sov. Phys. Usp **30**, 851 (1987)].
[138] A. V. Andreev, V. I. Emel'yanov, and Yu. A. Il'inskiĭ, Cooperative Phenomena in Optics [in Russian], Nauka, M., 1988.
[139] L. D. Landau and E. M. Lifshitz, *Quantum Mechanics*, 3rd ed. Pergamon Press, Oxford, 1977. [Russ. original, Fizmatgiz, M., 1968].
[140] M. Hillery *et al.*, Phys. Lett. A **103**, 259 (1984).
[141] M. I. Rabinovich and S. I. Trubetskov, *Introduction to the Theory of Oscillations* [in Russian], Nauka, M., 1984.
[142] B. Ya. Zel'dovich and D. N. Klyshko, Pis'ma Zh. Eksp. Teor. Fiz. **9**, 69 (1969) [JETP Lett. **9**, 40 (1969)].
[143] J. Neukammer *et al.*, Phys. Rev. Lett. **59**, 2947 (1987).
[144] I. M. Beterov, G. L. Vasilenko, and N. V. Fateev, Kvant. Elektron. (Moscow) **15**, 1488 (1988) [Sov. J. Quantum Electron. **18**, 933 (1988)].
[145] D. J. Heinzen and M. S. Feld, Phys. Rev. Lett. **59**, 2623 (1987).
[146] I. M. Beterov, I. I. Ryabtsev, and N. V. Fateev, Pis'ma Zh. Eksp. Teor. Fiz. **48**, 181 (1988) [JETP Lett. **48**, 195 (1988)].
[147] J. Krause, M. O. Scully, and H. Walther, Phys. Rev. A **36**, 4547 (1987).
[148] A. Heidmann and J. M. Raimond, Opt. Commun. **54**, 189 (1985).
[149] K. L. Kien, E. P. Kadantseva, and S. Shumovsky, Physica B + C **150**, 447 (1988).
[150] V. A. Andreev and P. B. Lerner, Phys. Lett. A **134**, 507 (1989).
[151] A. J. Lichtenberg and M. A. Lieberman, *Regular and Stochastic Motion*, Springer Verlag, Berlin, 1983. [Russ. transl. Mir, M., 1984].
[152] G. Casati, I. Guarneri, and D. L. Shepelyansky, IEEE J. **QE-24**, 1420 (1988).

[153] D. L. Shepelyansky *et al.*, Phys. Rep. **154**, 78 (1987).
[154] I. M. Lifshitz, S. A. Gredeskul, and L. A. Pastur, *Introduction to the Theory of Disordered Systems* [in Russian], Nauka, M., 1982.
[155] M. V. Fedorov, J. Opt. Soc. Am. B **5**, 53 (1988).
[156] M. Yu. Ivanov, *Elementary Processes in a Laser Radiation Field* [in Russian], Vysshaya shkola, M., 1987, p. 33.
[157] J. Mantica, IEEE J. Quantum Electron. **24**, 1453 (1988).
[158] L. Moorman, E. J. Galvez *et al.*, Phys. Rev. Lett. **61**, 771 (1988).
[159] T. F. Gallagher *et al.*, Phys. Rev. A **37**, 1527 (1988).
[160] J. Hare, M. Gross, and P. Goy, Phys. Rev. Lett. **61**, 1938 (1988).
[161] D. Delande and J. C. Gay, Europhys. Lett. **5**, 303 (1988).
[162] E. J. Galvez *et al.*, Phys. Rev. Lett. **51**, 2011 (1988).
[163] B. J. Hughey *et al.*, *Abstracts of the 11th International Conference on Atomic Physics*, edited by S. Haroshe and P. Goy, Paris (1988), p. VIII-38.
[164] J. E. Bayfield and D. W. Sokol, Phys. Rev. Lett. **61**, 2007 (1988).
[165] V. P. Chebotayev *et al.*, Appl. Phys. **9**, 171 (1976).

Translated by M. E. Alferieff